Title
ELECTRON MICROSCOPY AND ELECTRON DIFFRACTION OF FROZEN, HYDRATED BIOLOGICAL SPECIMENS

Author
Taylor, Kenneth A.

Publication Date
1975-04-01

LBL-2869

ELECTRON MICROSCOPY AND ELECTRON DIFFRACTION OF FROZEN, HYDRATED BIOLOGICAL SPECIMENS

DONNER LABORATORY

Kenneth A. Taylor
(Ph. D. thesis)

April 1975

Prepared for the U. S. Energy Research and Development Administration under Contract W-7405-ENG-48

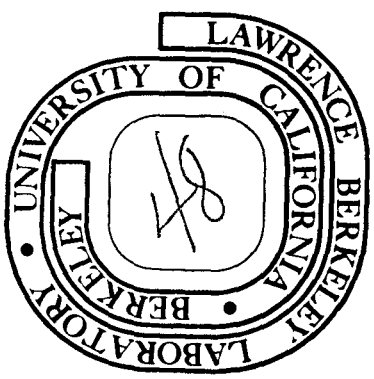

LBL-2869

DISCLAIMER

TABLE OF CONTENTS

ELECTRON MICROSCOPY AND ELECTRON DIFFRACTION OF FROZEN, HYDRATED BIOLOGICAL SPECIMENS

Kenneth A. Taylor

Donner Laboratory

and

Lawrence Berkeley Laboratory
University of California
Berkeley, California 94720

ABSTRACT

A method has been developed for the study in the electron microscope of frozen, unstained, hydrated biological specimens. Methodology is described for the preparation of frozen, sandwiched specimens and for their introduction into the electron microscope. Electron diffraction was used to show excellent preservation of crystalline structure in the frozen state. The radiation damage effect in frozen, hydrated specimens was measured. When the critical exposure for complete fading of the electron diffraction from frozen, hydrated catalase is compared with similar values reported in the literature for hydrated catalase at room temperature, an approximately ten fold improvement is seen for the frozen catalase crystals.

Techniques for obtaining images of frozen, hydrated specimens are described. Lattice images of unstained catalase crystals have been obtained, which extend to 21Å resolution. Contrast in unstained, hydrated catalase crystals has been measured by scanning densitometry and found to be greater than 10%.

I. INTRODUCTION

The prevention of the dehydration of biological specimens in the electron microscope has been a goal of microscopists for many years. There are two major reasons for this. Of primary importance is the desire to maintain the structure of the specimen to as high a resolution as possible and at the same time to minimize the production of artifacts due to the various specimen preparative procedures. Secondly, though not directly related to the hydration problem itself, is the desire to study the structure of the specimen and not the structure of the supporting matrix of heavy atom stain.

Throughout the history of electron microscopy there have been attempts to develop methods for maintaining the hydration necessary for biological specimens. These attempts did not meet with overwhelming success, and for this reason, the field turned instead to techniques that would preserve the structure of the specimen without maintaining its hydration. The most notable of these are the techniques of thin sectioning and negative staining. In addition, freeze drying and critical point drying techniques have been employed for preparing specimens which could otherwise be distorted by surface tension effects when dryed in air.

The primary drawback of techniques for preserving specimen structure without maintaining specimen hydration is the fact that they do not preserve periodic structure to its full high resolution state or, even more seriously, they may alter the structure. Langer et al. (1974) and Hoppe et al. (1968) have shown by x-ray diffraction techniques, that the periodicity of certain protein crystals was reduced to about 8Å after they had been aldehyde fixed, dehydrated and embedded in various polymerizing agents.

This is a significant reduction in diffraction resolution for it is known that fully hydrated protein crystals can diffract x-rays to resolutions often greater than 2Å and that image resolutions of about 5Å are necessary to visualize secondary structure in protein molecules. In addition, studies by Moretz et al. (1969a, b) have demonstrated that following fixation, dehydration and embedment of myelin, not only is the lattice dimension reduced but also the relative intensities are altered. These changes are strong evidence of the production of an artifactual structure.

Of all the specimen preparative techniques in use in biological electron microscopy, negative staining has perhaps had the greatest impact on structural studies at the macromolecular level. In this technique it is commonly thought that the primary purpose of the negative stain is to produce contrast in the image. While negative stains composed of atoms of high atomic number (heavy atoms) do increase the contrast, their most important function may instead be to support the structure during drying. Catalase can be used as an example. When dried without the use of a negative stain there is no periodic structure preserved as is evidenced by the complete loss of electron diffraction intensities. When dried in the presence of a negative stain such as uranyl acetate, electron diffraction intensities, in rare cases, can be seen to extend to 8Å (Glaeser, 1971). But if catalase is observed in the fully hydrated state, at room temperature, electron diffraction intensities can be observed at 2Å resolution (Matricardi et al., 1972).

The preservation of structure using a heavy atom stain is not achieved without paying a price. Because of the much higher scattering power of the heavy atoms relative to the atoms making up the biological material, their

contribution to the image contrast will be much higher than that of the organic material. Thus the image must be interpreted in terms of the distribution of the stain rather than the structure of the biological specimen. For this reason the most information one can hope to obtain from a negatively stained micrograph is an outline of the biological specimen.

However, without the use of negative stains, the number of isolated biological materials that can withstand dehydration in air without apparent structural changes is known to be very small. The purple membrane of Halobacterium Halobium is the only known case of an isolated lipid-protein membrane that can be successfully dehydrated. Both high resolution electron diffraction patterns and high resolution electron microscope images (Unwin and Henderson, 1975) have been obtained for this structure in the dried state. The various structural, fibrous proteins such as keratin, collagen or silk and certain synthetic peptides are the only known protein structures that can be successfully examined in a dehydrated condition (Parsons and Martius, 1964; Fraser and MacRae, 1973). Finally, Parsons (1966) has reported that helical diffraction can be obtained from a synthetic polymer of riboadenylic acid when it has been air dried. This is the only known case of a nucleic acid that maintains its helical structure on drying.

Because of the limited number of unstained specimens that can retain their structure on dehydration, the importance of maintaining hydration in the study of unstained specimens becomes apparent. It should be mentioned at this stage, that it might be possible to avoid the necessity of maintaining specimen hydration and at the same time satisfy the requirement

of using unstained specimens by resorting to the use of a sustaining matrix of a low molecular weight organic molecule. Some work of this type has been reported by Unwin and Henderson (1975) who have obtained high resolution electron diffraction patterns of catalase embedded in a 1% glucose solution.

There have been many previous attempts at maintaining specimen hydration in the electron microscope. These attempts have, for the most part been confined to room temperature techniques. These fall into two basic categories: the closed cell-thin window chambers and the differentially pumped hydration stages. Rather than attempt an exhaustive review of these techniques, I will merely outline their features here and discuss the most notable results that have been obtained. The interested reader is referred to the reviews by Parsons (1974), Parsons et al. (1974), and Joy (1972) for a more extensive discussion.

The oldest attempts at maintaining specimen hydration used the closed cell-thin window chambers. With these devices, the specimen area is usually isolated from the microscope vacuum by two thin windows. These windows have been made of a variety of materials of various thicknesses. The dimensions of the chambers have also varied. Some successes have been claimed for such chambers but in general the claims have not been reproduced by other workers. There are two major problems with such an approach. If the windows are not made thick enough, they tend to break and water is lost. On the other hand if they are made too thick, the scattering from them causes loss of image contrast. These difficulties can in principle be overcome using a high voltage microscope and this has resulted in a revived interest in the use of these chambers for such

microscopes.

The most dramatic success in maintaining specimen hydration in the electron microscope was achieved by Parsons and co-workers using the differentially pumped hydration stage. The differentially pumped stage differs from the closed cell thin window chambers in that the specimen is not isolated from the microscope vacuum. Instead, a series of four colinear apertures are used in conjunction with differential pumping. Between the middle two apertures is the specimen area. Water vapor or a suitable carrier gas saturated with water vapor is introduced into this area and leaks out into the upper and lower pumping chambers located between the first and second apertures and the third and fourth apertures. Success or failure of this dynamical system depends on precise regulation of temperature and flow rate of the water vapor. If the specimen is colder than the temperature of the water vapor, then condensation occurs. This increases the specimen thickness and decreases the contrast in the image in addition to causing an increase in the background scattering in the electron diffraction pattern. Of course if the specimen is warmer than the temperature of the water vapor being introduced then the specimen dries out. That these seemingly insurmountable technical difficulties have indeed been overcome was demonstrated when Matricardi et al. (1972) succeeded in obtaining high resolution electron diffraction patterns from unstained, unfixed catalase crystals. Catalase crystals are an ideal specimen for such a demonstration because at less than 95% relative humidity no diffraction can be obtained from the crystals (Longley, 1967). In addition to electron diffraction patterns from protein crystals, Hui and Parsons (1974) have reported obtaining electron diffraction patterns from

wet, human erythrocyte membranes. It should be noted that results similar to those of Matricardi et al. have not been reported for the closed cell-thin window environmental chambers.

The use of room temperature hydration stages has one serious drawback. Brownian motion of colloidal particles is severe at room temperature. This problem has been aptly described by Abrams and McBain (1944), who wrote,

> "The problem of observing Brownian movement of ordinary particles such as gold in the electron microscope is similar to that of photographing a fly in a living room with a time exposure."

The importance of Brownian motion should be qualified somewhat. First of all whole cells and large, in the electron microscopical sense, protein crystals most likely do not exhibit Brownian movement in room temperature hydration stages. Whole cells grown on specimen grids adher to the support films. Protein crystals would not exhibit Brownian motion unless suspended in a very thick film of water. The problem is likely to be very severe, however, for membranes and free standing particles like single viruses. Moreover while whole cells themselves will not show Brownian motion, their cytoplasmic components will not be restricted. To overcome the Brownian motion problem Parsons et al. (1974) have proposed a form of flash microscopy which would utilize a flash of high intensity electrons and a very short exposure time. However they have not produced any positive results to date.

The prevention of Brownian motion is complete when the specimen is frozen. This is one of the reasons that work has proceeded toward the

development of frozen specimen hydration techniques. In addition to this thesis, work has been reported by Heide and co-workers on frozen specimen techniques. In addition to eliminating the Brownian motion problem, the frozen specimen techniques have further advantages. First, specimen support films can be very thin or even non-existent with frozen specimen techniques, because the film of ice can act as its own support film. Second, the equipment requirements are modest in comparison to either the closed cell thin window chamber or the differentially pumped stages. All that is required is a cold stage and methodology for the introduction of frozen specimens into the microscope. There are some potentially major drawbacks however. Most important of these is the danger of ice crystal damage occurring to the specimen during freezing. However, as will be shown, this is not a problem for specimens of the type used here. Secondly, there could also be a problem with sublimation of the ice, which in effect would freeze dry the specimen. This also is not a problem in the frozen thin sandwich technique.

II. THE METHODOLOGY OF THE FROZEN SPECIMEN TECHNIQUE

A. The Preparation of Thin Hydrophilic Support Films

The preparation of hydrated specimens, either in the liquid state or frozen state requires a support film that has a hydrophilic character. This hydrophilic character is necessary because of the property of water droplets to bead up on a hydrophobic surface. This can yield a specimen which is surrounded by a thick film of water. This would cause a reduction in image contrast and an increase in background scattering in the electron diffraction patterns. Hydrophilic support films can be produced by glow discharge treatment of a hydrophobic carbon film. This method is often unreliable and, in addition, the hydrophilic films, when produced, do not retain their hydrophilic character during storage. Adsorption of hydrophilic organic compounds can render a support film hydrophilic. However the films produced by this method have an unknown thickness and composition.

To avoid these drawbacks a method was developed for producing hydrophilic support films by depositing SiO onto thin carbon support films. Silicon monoxide has been used in electron microscopy for many years. It is a completely amorphous material whose electron diffraction pattern shows only diffuse rings (Hass, 1950). It has a low vaporization temperature which makes it ideal for vacuum deposition. In addition deposited films are optically transparent, which provides for an easy method of measuring the thickness of the deposited film. SiO has the disadvantage in that it is a stronger scatterer of electrons than carbon.

Specimen support films for use with frozen specimens are prepared by vacuum depositing about 50Å of carbon onto the formvar side of a

formvar coated 200 mesh folding grid. The formvar film, which is about 300Å thick, is then removed by suspending the grids for 15 minutes in a beaker of ethylene dichloride (Bradley, 1965). The procedure is to touch the carbon coated formvar grid, formvar side down, to the surface of a shallow beaker of ethylene dichloride for one or two seconds. When dried, the step is then repeated once more after which the grids can be suspended in a beaker of fresh ethylene dichloride. This procedure has been used because the coverage of the windows of the grid by the carbon films is better than if a floating carbon film is picked up from the water. Good coverage is necessary because when the specimen is produced the grid is folded in two, and this results in the fraction of "sandwiching" windows being the product of the fraction of carbon coated windows on the two faces.

Silicon monoxide is vacuum deposited directly onto the thin carbon support film using the rotating shutter device shown in Fig. 1. The carbon grids are placed on a circular disk which rotates under a stationary table. This table has a slot cut in it such that each grid is exposed to the SiO source for only 5% of the period of evaporation. The thickness of the film deposited on the grid can be monitored by simultaneously condensing a much thicker film of SiO onto a clean glass slide or piece of reflecting metal (Williams, 1973). The glass slide is placed much closer to the SiO source in order to form an optical wedge of sufficient thickness to observe interference colors in reflected light. From the color, interference order, index of refraction (Siddal, 1960) and geometry the thickness of the SiO film deposited on the specimen grid can be calculated. This calculation assumes a point source of SiO and is thus valid

Figure 1. Schematic diagram of the rotating shutter device for vacuum depositing SiO onto specimen grids. A large number of specimen grids are placed on the disk which is rotated at 300 rpm. Each grid is repeatedly brought in turn under the slot in the stationary table, and is thereby exposed to the source of SiO for only 5% of the period of evaporation. Interference colors produced on a glass slide or polished metal plate serve as a reference for judging the film thickness.

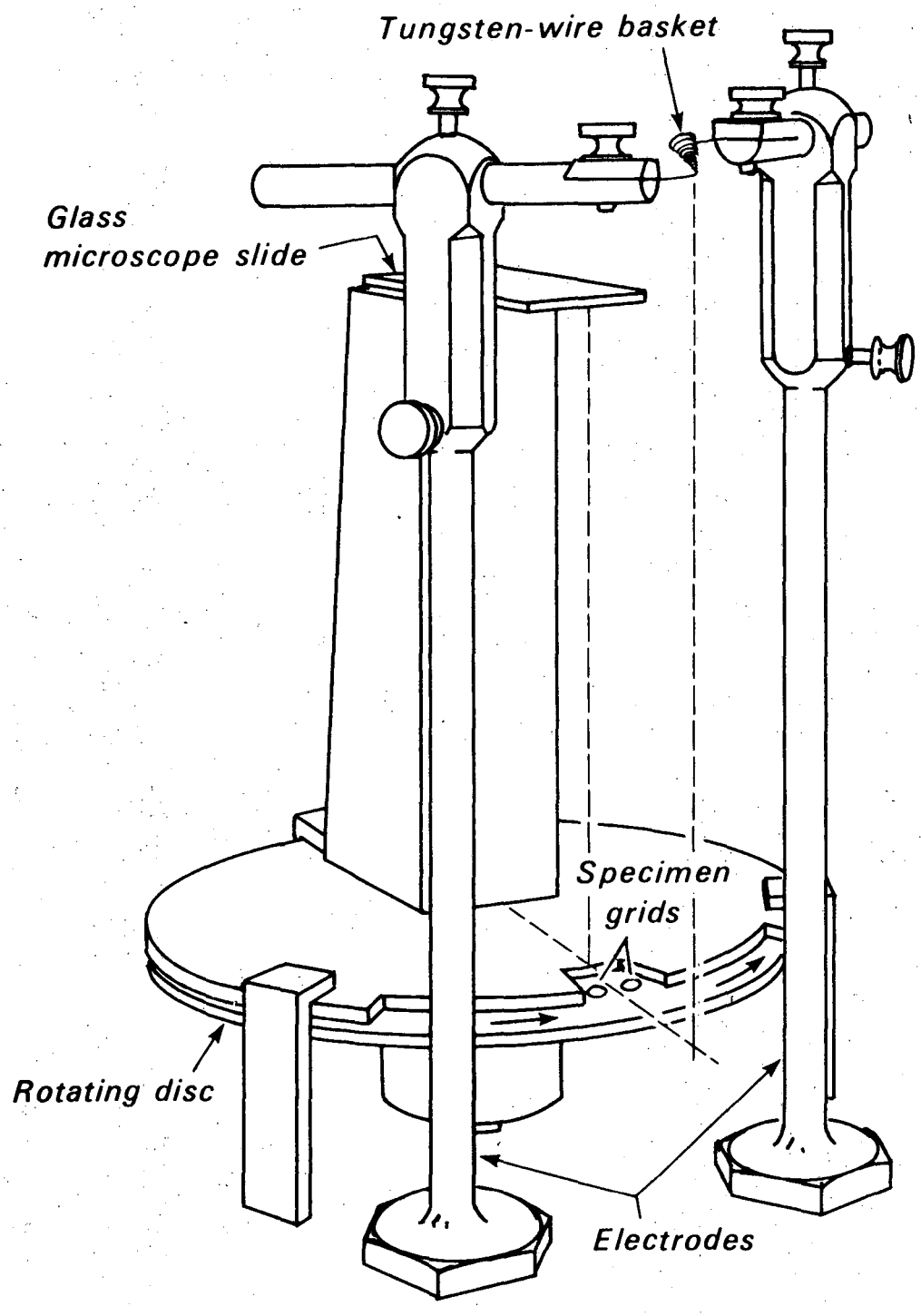

Fig. 1

DBL 734-5132

for distances large compared with the extension of the source. This condition is satisfied because the distance between the SiO source and the specimen grids is 16.5 cm whereas the extension of the SiO source is only 0.5 cm.

The determination of the thickness of deposited SiO which will render a carbon film hydrophilic is necessarily empirical. A simple test for determining if a support film is hydrophilic can be made by touching a droplet of water to the side of the grid. The drop will spread out over the grid if the support film is hydrophilic but will remain as a rounded droplet if the support film is hydrophobic. Using this test a measured layer thickness of 10Å to 15Å will render a carbon film hydrophilic for the production of thin aqueous films. The thickness of the thin carbon films can be as low as 5-10Å if a secondary reticulate support film is used (Williams and Glaeser, 1972). Carbon films of thickness 40-60Å can be used as entirely self supporting films on 200 mesh copper grids. Thus, total support film thicknesses for the sandwiched specimens is about 100-150Å when self supporting carbon films are used and can be as low as 50Å when secondary reticulate films are used.

Another simple test that can be used to determine that vacuum deposited films of SiO are indeed hydrophilic can be made by taking four clean glass slides (cleaned in dichromate-sulfuric acid cleaning solution) and coating them with various support film materials. One of the glass slides is coated with a thick film of formvar, another with a thick film of carbon, the third with a thick film of SiO and the other left untouched. When drops of water of equal volume are placed on each film, the drop will bead up on the formvar and carbon films and spread out equally well

on SiO or the clean glass.

B. The Preparation of Frozen Specimens

Heide and Grund (1974), have proposed a novel method for the preparation of frozen, thin specimens for electron microscopy. This method uses a small diameter ring of a thin wire which is dipped into the specimen and then frozen in liquid nitrogen. With this technique there is no specimen support film. For the purpose of this study, it was found more convenient to use specimens which were sandwiched between thin hydrophilic support films. The sandwiching method is advantageous because it reduces the surface area available for sublimation of the ice. Sandwiching also helps to produce thin aqueous films by virtue of the effect of surface tension acting on the hydrophilic sandwiching films.

Several techniques for producing frozen thin sandwiches were tried. Initially, individual 200 mesh copper grids which were coated with thin composite, hydrophilic support films were used for the sandwiching. The sandwiching was accomplished by placing a drop of specimen on the face of one of the grids and then placing the other grid, face down on top of the drop of specimen. The excess water could then be withdrawn with filter paper leaving the two grids sandwiching the film of water. These were then plunged directly in liquid nitrogen.

Satisfactory thin films of ice could be produced in this manner. However, the method was less than perfect because the bars of the upper and lower specimen grids were often not in register. This of course, resulted in a reduction in the size of the specimen windows. In the course of many experiments, it was found that the ice films were often thickest near the grid bars and thinnest in the center of the windows.

For this reason it was felt that, if sandwiches could be produced using two hydrophilic films but only one specimen grid, uniformly thin films of ice could be produced.

In principle this idea can be achieved by floating a composite film of SiO and carbon on a water surface and then picking the film up, SiO face to SiO face, with a grid which also has a composite film mounted on it. The composite films for flotation can be produced by first vacuum depositing carbon onto a freshly cleaved mica surface and following that with a deposition of SiO onto the carbon. It is important to leave the leading edge of the carbon film free of SiO in order to achieve separation of the carbon film from the mica surface. As these films are brittle they can be broken into appropriate size and picked up with the 200 mesh grid.

Using grids prepared in this way, the specimen can be sandwiched simply by touching a drop of specimen to the edge of the grid. The droplet promptly spreads out between the two SiO films. The second sandwiching film can be seen, in reflected light, floating on the surface of the water droplet. By carefully touching a torn piece of filter paper to the edge of the grid, most of the excess droplet can be removed. Specimens prepared in this manner were unsatisfactory because, instead of having uniformly thin films of ice, uniformly thick films were obtained. The reason for this is probably that the film thickness reaches a point where the filter paper is no longer effective at withdrawing excess water and that this thickness is too great for use in the electron microscope.

A third method, the one for which the greatest success was achieved,

employed the use of folding grids. The procedure is illustrated in Fig. 2. The 200 mesh folding grid is folded partially in half (Fig. 2a). A drop of specimen sufficient to fill the space between the two films is added and left for a period of several minutes (Fig. 2b). This waiting period gives the specimen time to adhere to the support film. The two halves of the grid are then folded tightly together and the excess fluid is withdrawn with a torn piece of filter paper (Fig. 2c). The grid is then plunged directly into liquid nitrogen (Fig. 2d). Experience has shown that steps a and c, the initial folding of the grid and the withdrawal of the excess fluid, are the most important for the production of thin aqueous films. If the grid is not folded carefully the grid bars will not be properly aligned and the window size will be reduced. If the excess water is not withdrawn carefully thick films are produced. It is believed that the careful withdrawal of the water, coupled with the adherence of the water to the hydrophilic support films, produces the thin aqueous films.

When a drop of distilled water is used as the specimen, two types of ice films, uniform sheets and microdroplets, are usually produced. Fig. 3 shows an extensive area of thin ice covering the entire window of a 100 mesh folding grid. Bend contours and grain boundries can be seen, demonstrating crystallinity which has been unequivocally proven through electron diffraction. Fig. 4 shows an area of microdroplets. The large extension of the drops and their relative transparency to electrons indicates that they have indeed spread out or wetted the hydrophilic surface of the support films before freezing. Again grain boundries and bend contours can be seen in the ice thus demonstrating crystallinity. The position of the bend contours can be observed to vary with time depending

Figure 2. Procedure for producing frozen thin specimens for electron microscopy. (a) A 200 mesh folding grid is folded in two partially. (b) A drop of a suspension of specimen sufficient to fill the space between the two faces of the grid is applied. (c) The two faces of the grid are folded tightly and the excess fluid is withdrawn with filter paper. (d) Specimen is immediately frozen by plunging into liquid nitrogen. The grid is placed in the specimen holder cap. The cap is mounted upright in a brass block which is also submerged in liquid nitrogen. The cap with specimen is mounted on the specimen holder and then placed in the cold sink-frost protector for transfer into the microscope.

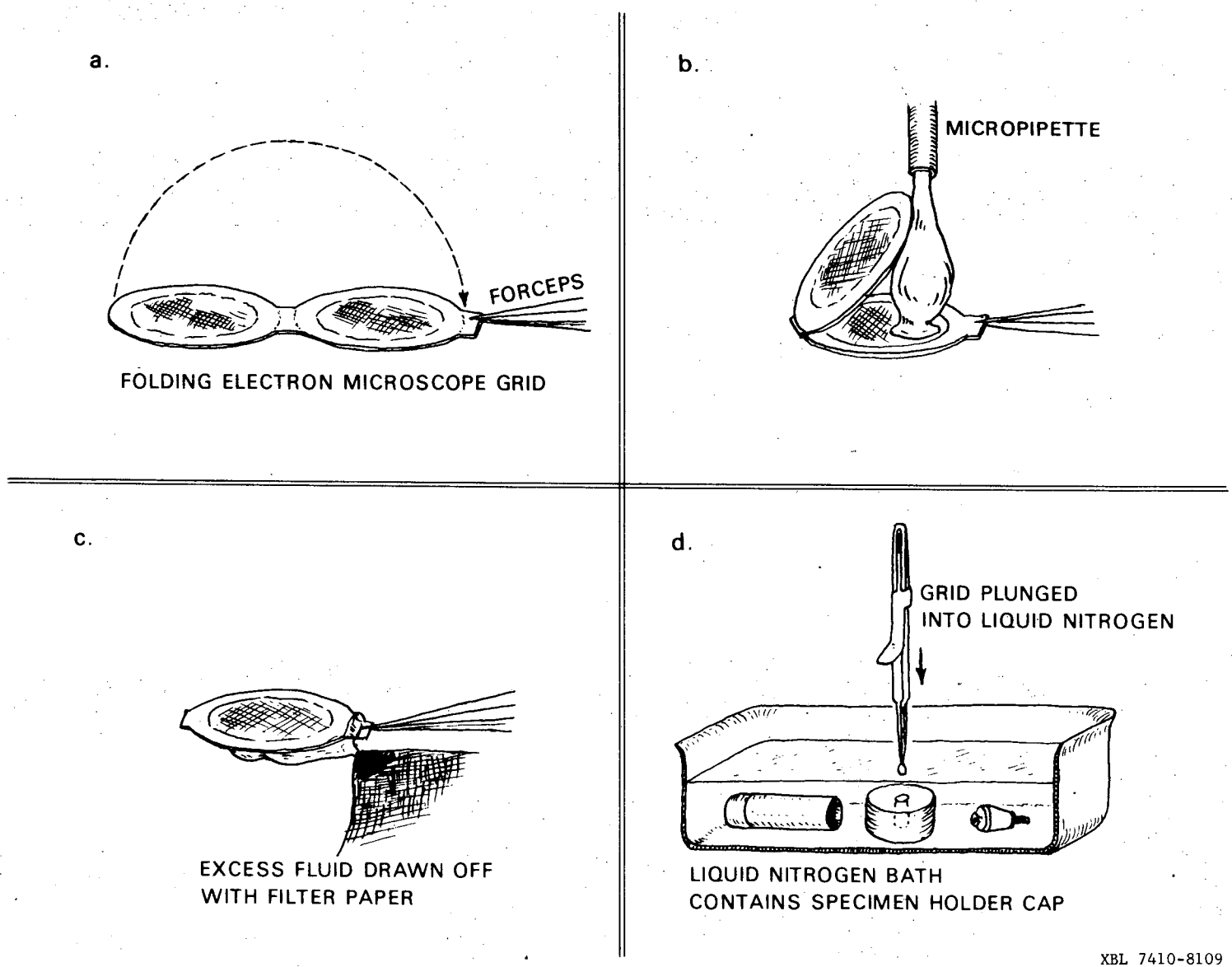
a.
FORCEPS
FOLDING ELECTRON MICROSCOPE GRID
b.
MICROPIPETTE
c.
EXCESS FLUID DRAWN OFF
WITH FILTER PAPER
d.
GRID PLUNGED
INTO LIQUID NITROGEN
LIQUID NITROGEN BATH
CONTAINS SPECIMEN HOLDER CAP
XBL 7410-8109

Fig. 2

Figure 3. Electron micrograph of an extensive film of ice prepared from distilled water. Thickness and extension of the ice can vary. Bend contours and distortions in the ice are observed to change with time under the influence of the electron beam.

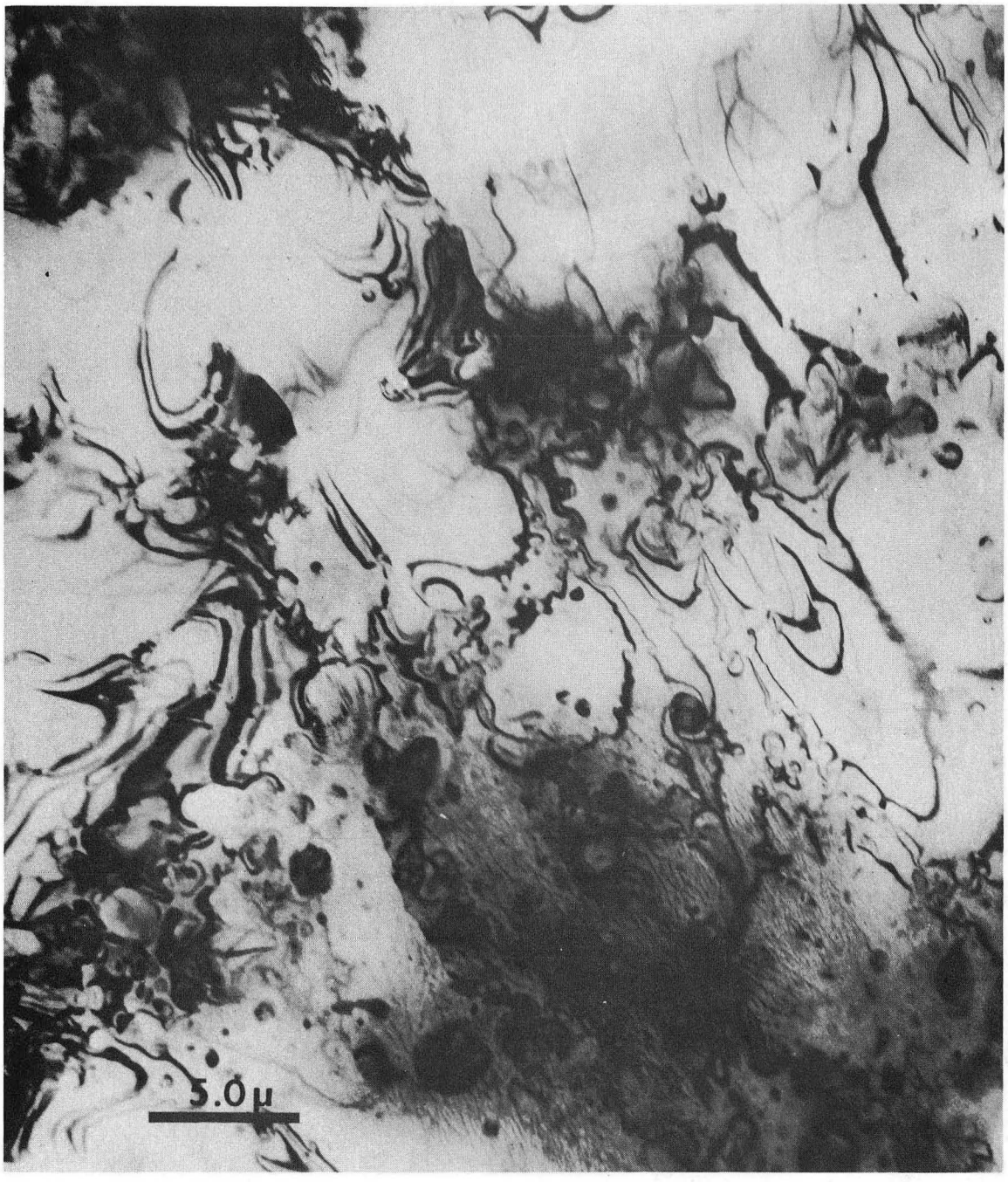

XBB 751-846

Fig. 3

Figure 4. An area of frozen microdroplets of ice prepared from distilled water.

XBB 751-849

Fig.4

upon the intensity of illumination. This is an indication that some distortion of the specimen is occurring due to the electron bombardment.

These films of ice are relatively stable with respect to sublimation. Specimens have been observed for several hours without visible loss of water. However, when an intense beam of electrons is focused onto the specimen, the ice can be seen to sublime.

C. The Introduction of Frozen Specimens Into the Microscope

Once the frozen thin sandwich specimens are produced, it is necessary to introduce them into the microscope without frost forming on the specimen and without substantial warming of the specimen. To accomplish this purpose, Heide and Grund (1974) have proposed a "diving bell" type of apparatus. With this method the frozen specimen is first mounted in the specimen holder under liquid nitrogen. The specimen holder is then placed, under liquid nitrogen, in the "diving bell" which was previously filled with gaseous nitrogen. The "diving bell" is then closed off with a plug, which has a narrow channel winding about the base to allow for evacuation of the inside of the chamber but which, because of the dimensions of the channel, does not permit water molecules to diffuse into the chamber. The closed "diving bell" can then be placed into the airlock port and the airlock evacuated.

In the work of this thesis the problem of frost formation and specimen warming was solved by the use of cold sink-frost protector. A quite simple apparatus of this type was constructed for the Hitachi HU-11 electron microscope (Taylor and Glaeser, 1973) and is shown in Fig. 5. The cold sink frost protector consists of a copper bar which has been machined hollow and conforms to the taper of the specimen holder. The specimen

holder can be placed into the cold sink frost protector under liquid nitrogen and then transferred to the airlock port of the electron microscope in a plastic plug. The plug, in addition to serving as a transfer mechanism for the frost protector and specimen holder, also serves as a vacuum seal for the airlock during evacuation and specimen exchange. After the airlock is evacuated the specimen holder is then transferred to the cold stage with the conventional specimen exchange device.

The same basic principle of the cold sink-frost protector can also be incorporated into a technique for introducing frozen specimens into the JEM 100B electron microscope. Although the method of exchanging specimens in the JEM 100B is more complicated than in the Hitachi HU-11, the only adaptation that is necessary is to modify the airlock door so that it can accept the cold sink frost protector when the specimen holder is mounted in it. Specimen exchange can then be accomplished in the conventional manner. Many of the other design features of the conventional airlock door were incorporated into this modified apparatus.

Fig. 6 is a drawing of the airlock door modification for the JEM 100B. The airlock door consists of a body of nickel plated brass and a rotating stainless steel drum. Machined into the drum are two positions for mounting the frost protector, specimen holder combination and one position for receiving the cold specimen holder from the microscope column. Stainless steel was used for the rotating drum, for two reasons. In the first place it is more durable than plastic and in the second place it has a very low thermal conductivity for a metal. Its thermal conductivity is greater than that of the available plastics but this can work as an advantage because of the undesirability of placing on the cold stage, a

Figure 5. The modified airlock plug for introducing frozen specimens into the Hitachi HU-11 electron microscope. (a) The three individual components. From left to right they are the plastic airlock plug, cold sink-frost protector, and specimen holder. The specimen holder is placed in the frost protector under liquid nitrogen and the combination can then be mounted in the airlock plug as shown in (b).

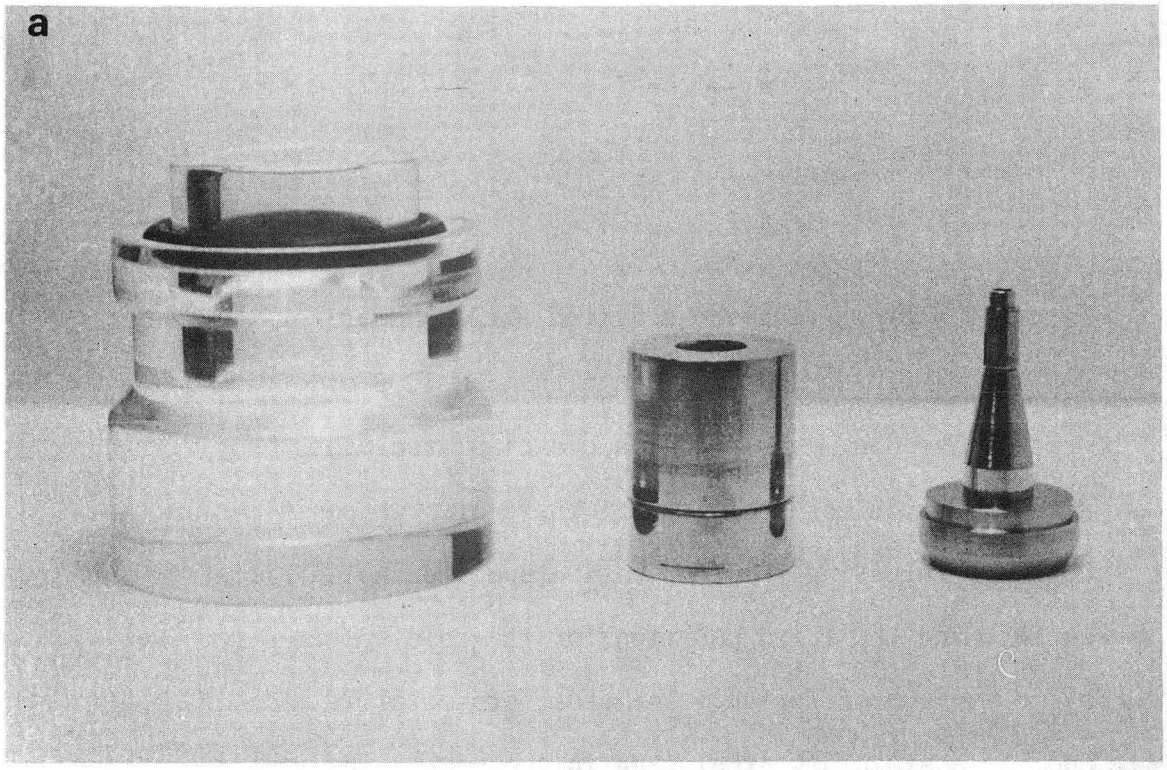

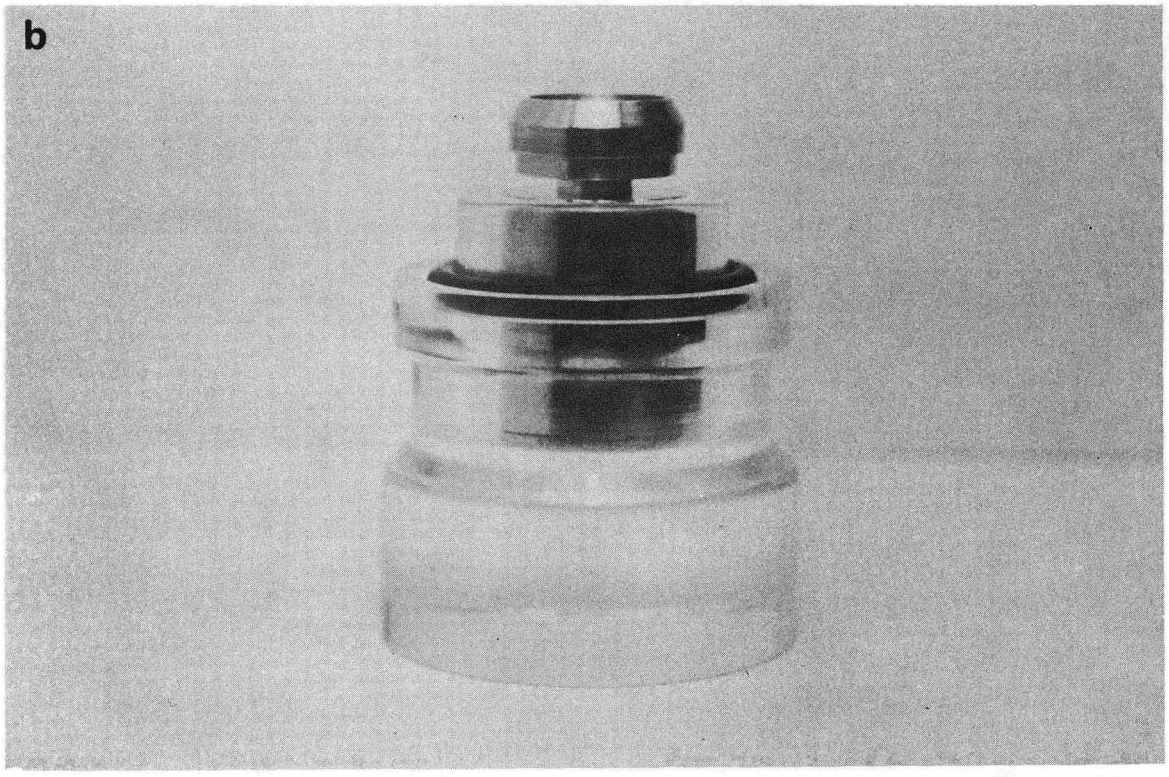

Fig. 5

XBB 751-847

Figure 6. Drawing of the modified airlock door for the introduction of frozen specimens into the JEM 100B electron microscope. The door consists of a nickel plated brass body with a rotating stainless steel drum. There are two positions in the drum for receiving the combination specimen holder-frost protector, and the third position for the cold specimen receiver alone is made of Teflon. The frost protector is made of copper and has a stainless steel ring in the back. The inside of the frost protector is machined to conform to the taper of the specimen holder.

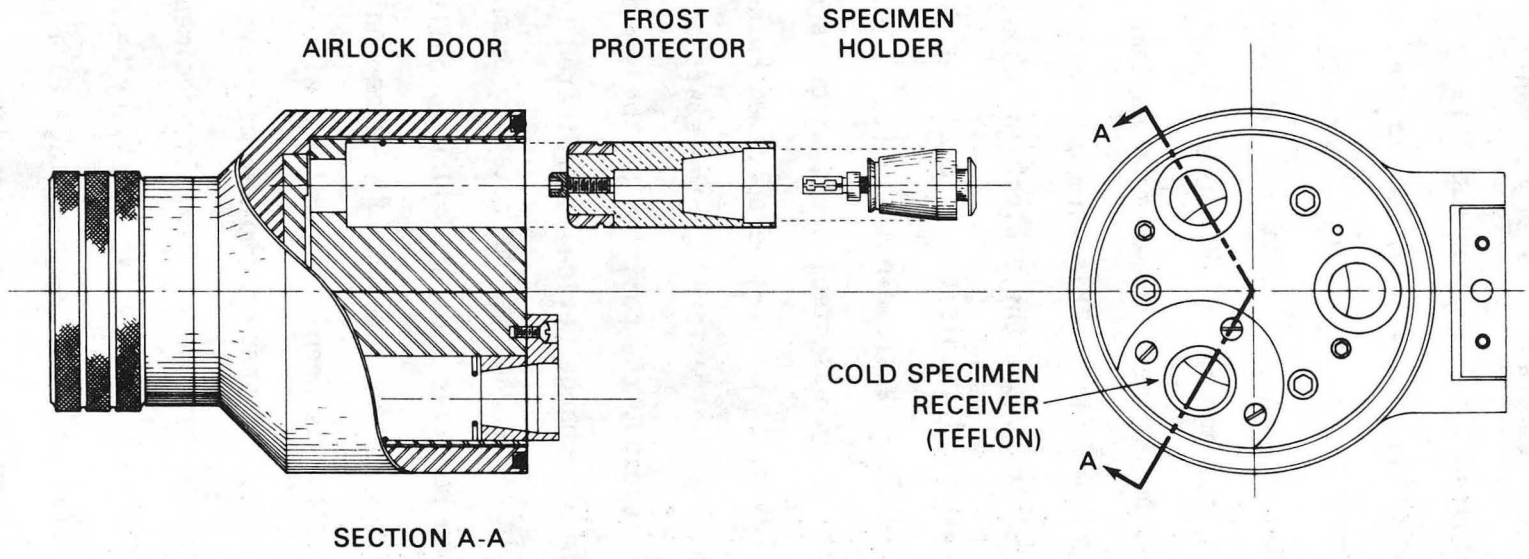
AIRLOCK DOOR
FROST PROTECTOR
SPECIMEN HOLDER
A
A
COLD SPECIMEN RECEIVER (TEFLON)
SECTION A-A
XBL 749-4948

Fig. 6

specimen holder whose temperature is significantly lower than that of the cold stage. The reason this is undesirable is that if the specimen holder is colder than the stage then it will expand when placed on the warmer stage and thus become locked or "frozen" onto the stage. Since the specimen holder has a temperature of -197° C when removed from the liquid nitrogen bath and the cold stage in the JEM 100B only attains a temperature of -120° C the specimen holder needs to warm up substantially before it can be safely placed on the stage. This warm up process is accomplished by keeping the specimen holder in the airlock for about 30 seconds. If a colder stage were available, this period could be shortened, or plastic might be substituted for the stainless steel.

Rotation of the stainless steel drum, which is necessary for the specimen exchange device to engage the specimen holder, is achieved by means of an aluminum handle fastened to the shaft of the drum. When the airlock door is closed, the position of the specimen holder with respect to the specimen exchange device is indicated by a spring loaded detent stop built into the back of the rotating drum.

A cold specimen receiver made of Teflon is built into the rotating drum for the purpose of accepting a cold specimen holder from the cold stage after observation has been completed. A wire spring in the back of the receiver engages the specimen holder to prevent if from falling out when the airlock door is opened. A cold specimen receiver of plastic or some other flexible material is necessary because the cold specimen holder, if transferred from the cold stage to a metallic receiver could expand during warming and become locked in.

The cold sink frost protector for the JEM 100B is made of copper

and has an inside taper which closely matches that of the specimen holder. At the back of the frost protector, on the outside, is a stainless steel ring with a circular groove cut in it. This groove engages another spring bearing built into the back of the rotating drum. The spring bearing and the circular groove in the stainless steel ring firmly hold the cold sink frost protector and prevent it from being drawn into the specimen chamber of the microscope along with the specimen holder.

III. RESULTS AND DISCUSSION

The usefullness of the frozen specimen technique for biological structure investigations depends on three quantities: (1) the degree of structural preservation in a frozen, hydrated specimen, (2) the effect of radiation damage on a frozen, hydrated specimen, and (3) the amount of contrast in an unstained, hydrated specimen. The first two quantities were easily measured by electron diffraction experiments. To measure the image contrast, however, required the development of some specialized techniques for obtaining images of frozen specimens.

A. Structural Preservation in Frozen, Hydrated Specimens

A large literature has been built up over the effects of freezing on biological tissue. The reader unfamiliar with this subject can refer to these references (Harris, 1964: Meryman, 1966; Smith 1961; Bullivant, 1970). The basic problem is one of ice crystal damage. This occurs when the intracellular water freezes into a crystalline form. These ice crystals can grow and coalesce thus disrupting the ultra-structure of the cell. Even if the intracellular water freezes into a vitreous or glassy form during freezing, a phase change in the ice can occur to the crystalline state if the specimen is warmed above the glass transition point which is about -130° C. Ice crystal formation can be prevented or at least kept to a tolerable limit through a combination of rapid freezing and the use of small hydrophilic organic molecules commonly referred to as cryoprotectants. In addition it is also common to use a saturated aqueous solution of chloroform which produces a large number of nucleating sites resulting in small crystals of ice being formed. It would be most desirable, however, to avoid the use of cryoprotectants in the preparation of frozen

specimens because of the possibility that they might cause alterations in structure. For this reason it was decided to freeze specimens directly in liquid nitrogen without using cryoprotectants.

Although one might think that freezing directly in liquid nitrogen would be quite rapid, in fact it is not because of the formation of an insulating layer of nitrogen bubbles. One of the most pessimistic findings with respect to freezing of protein crystals was the claim that freezing of protein crystals, of a size suitable for x-ray diffraction, in liquid nitrogen results in total disordering of them.

The disordering of large protein crystals when frozen in liquid nitrogen may be caused by the formation of crystalline ice rather than vitreous (glassy) ice. The formation of crystalline ice could disorder the crystal in two conceivable ways. First a volume change may occur in the aqueous phase of the crystal unit cell caused by crystalline ice expanding under conditions where vitreous ice would be contracting. Or, alternatively, the formation of crystalline ice could result in an effective dehydration of the protein due to water molecules, which were previously bound to the protein, being instead bound up in the ice lattice.

A somewhat more encouraging result for the freezing of biological specimens was reported by Dowell et al. (1962). Dowell et al. observed x-ray diffraction patterns from aqueous gelatin gels of various concentrations, frozen at different rates. They found that the cooling of a 50% gelatin gel at a rate of about 1°/sec prevented crystallization of the water. In addition, at a concentration of 58% gelatin, no crystalline ice was found regardless of the cooling rate. This is quite an encouraging result since most protein crystals have less than 50%, by volume, water

of hydration (Mathews, 1968) so that if the cooling rate was rapid enough, crystallization of ice might be prevented.

The whys and wherefores of structural preservation in frozen specimens become somewhat academic in the light of the electron diffraction results shown in Fig. 7. In Fig. 7 is shown an electron diffraction pattern of a frozen, unstained, unfixed catalase crystal in the hydrated state. The diffraction pattern on the plate extends to about 3Å while on the photographic print it extends to about 4Å. Diffraction patterns have been obtained to 2.5Å but do not reproduce well photographically. In addition to having been frozen directly in liquid nitrogen, these crystals have been embedded only in the solution from which they were crystallized and no cryoprotectants have been added. Thus it can be concluded from this result that a sufficiently rapid freezing rate is achieved in liquid nitrogen to prevent crystalline disordering in these specimens. This should not be too surprising because these specimens are very thin, only a few thousand Å compared to the 0.1 mm thick crystals used in x-ray crystallography, and the cooling rate could be quite rapid, even in liquid nitrogen.

Some ice crystal damage does occur but appears to be limited to the fragmentation of large crystals. This can be demonstrated by freezing catalase crystals in liquid nitrogen, thawing, and observing them in the electron microscope in the negatively stained state. For this experiment a drop of a catalase crystal suspension, of a concentration suitable for a negatively stained preparation was placed on a conventional formvar grid. The crystals were sometimes suspended in a 1% uranyl acetate solution and sometimes simply suspended in the solution from

which they were crystallized. There was no effect observable in the final result that could be attributable to the suspending solution. The grid was then frozen directly in liquid nitrogen, thawed, stained (if they were not already in stain), and dried. In the electron microscope, instead of the usual rectangular plates, fragments of plates could be observed. In some instances the fragments were deposited near one another and the fracture could be easily seen, as is shown in Fig. 8. However, even though the crystal has been fractured, its periodicity is intact in each of the fragments.

Two things should be pointed out with respect to the experiment described above. First, the damage could occur not only in the freezing step but also in the thawing step. The results of these two processes are indistinguishable in this experiment. Secondly, this gross fragmentation of large specimens may represent a limitation of the frozen specimen technique. Thus the larger the biological structure, the more likely that it will be damaged during freezing.

There is one anamoly that bears mention. While the periodicity of the catalase crystals is well preserved, the crystals themselves are still surrounded by bulk, crystalline ice. One explanation for this is that the ice freezes in a vitreous or glassy state and then crystallizes when the specimen warms from -197° C to about -120° C which is the temperature of the specimen stage in the microscope. The specimen temperature itself is likely to be somewhat warmer. It is unfortunate that this is the lowest temperature that the cold stage can attain because vitreous

Figure 7. Electron diffraction pattern of a catalase crystal which was frozen in liquid nitrogen and observed on a specimen stage cooled with liquid nitrogen. The resolution of the photographic reproduction is 4.5 Å, although that of the diffraction pattern on the original plate was 3.4 Å.

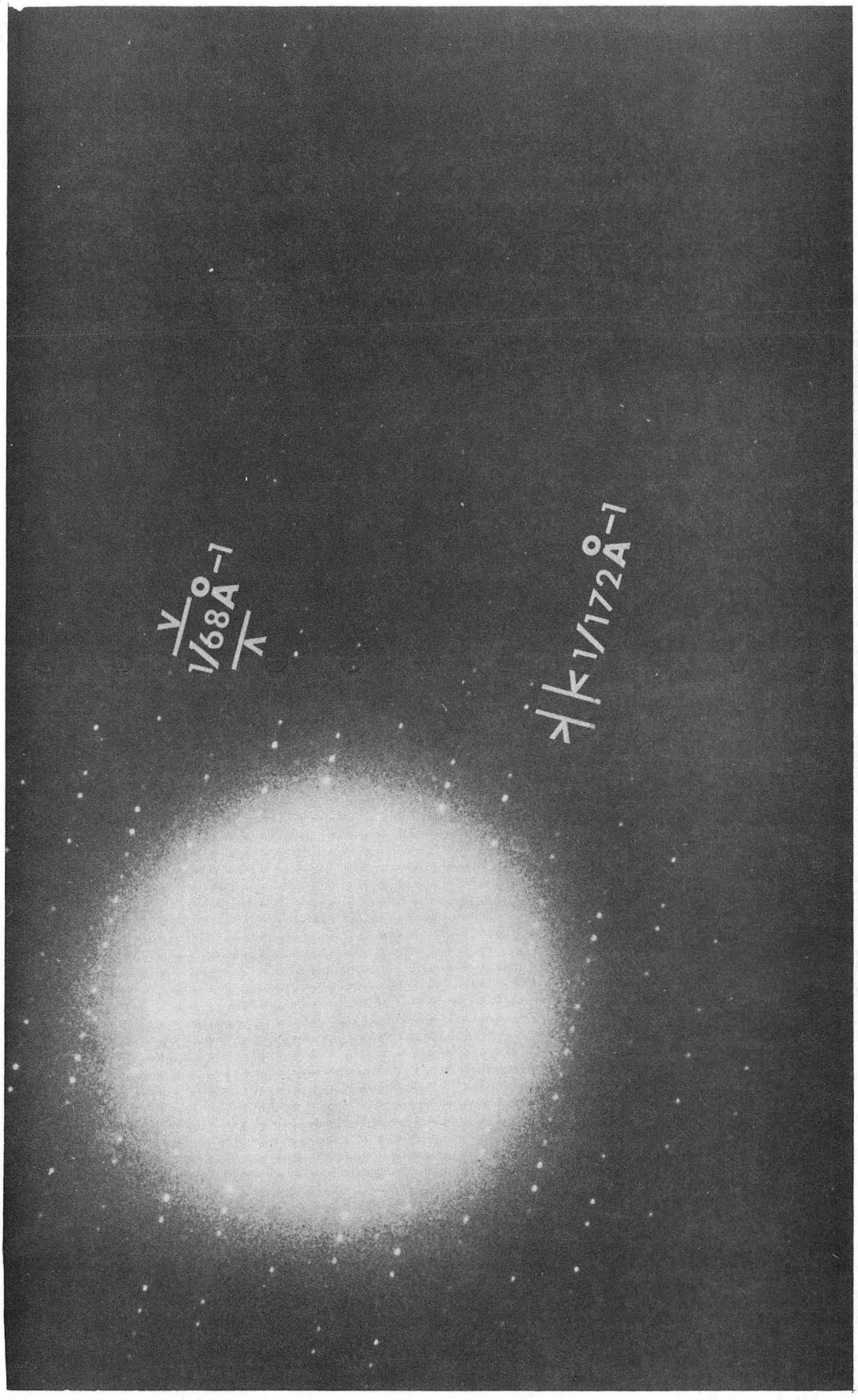

XBB 751-851

Fig. 7

Figure 8. Image of a negatively stained catalase crystal after one cycle of freezing and thawing on the specimen grid. The crystal has fractured and the pieces remained in close proximity. Despite the breakage, the periodicity of the crystal has been preserved in each of the pieces.

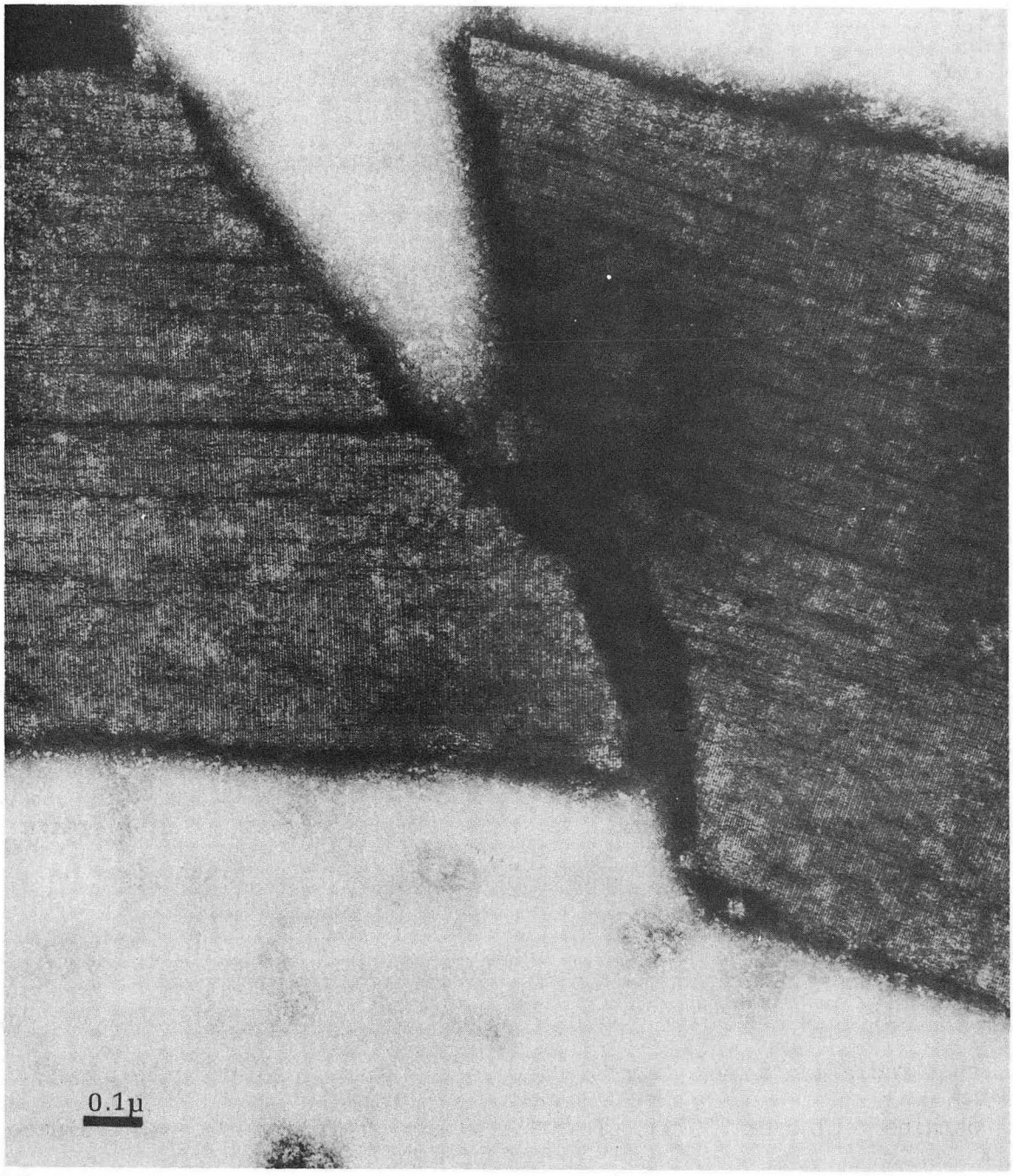

XBB 751-848

Fig. 8

ice can undergo a phase change to the crystalline state at temperatures between -130°C and -80°C (Blackman and Lisgarten, 1959). There is further experimental reason to believe that this is the explanation. Once, when using distilled water as the specimen, a thin film of apparently glassy ice was produced. It is here referred to as glassy or vitreous because it exhibited none of the diffraction contrast effects characteristic of crystalline ice films. However, when the electron beam was focused on this film, diffraction contrast effects suddenly appeared and began growing outward from the focused beam. Sublimation of the ice also occurred where the beam was brought to cross over. Dr. Heide also informs me that he has no difficulty preserving vitreous films on his cold stage which can reach temperatures as low as -188°C (Heide and Grund, 1974), well below the transition point for the phase change from the vitreous to the crystalline state. His specimens are also frozen directly in liquid nitrogen without the use of cryoprotectants.

B. Radiation Damage in Frozen, Hydrated Biological Specimens

It is a generally accepted fact of biological electron microscopy that radiation damage severely limits the image resolution that can be obtained (Glaeser, 1971). For this reason it is necessary to evaluate the sensitivity of frozen hydrated specimens to the electron beam. This can easily be done using electron diffraction, by measuring the resolution remaining in the diffraction pattern as a function of accumulated electron exposure. Here we define the critical exposure as the accumulated exposure of the specimen to electrons that will cause loss of

diffraction at a given resolution. Again catalase was used as the specimen. This is a favorable specimen choice because the results obtained can be directly compared with similar results for negatively stained catalase (Glaeser, 1971) and hydrated catalase crystals at room temperature (Matricardi et al., 1972).

In this experiment, electron exposures were measured with a lithium drifted silicon detector which was mounted in a specially constructed housing just below the final image plane of the electron microscope. The efficiency of this detector is estimated to be 60% for 100 keV electrons (Howitt, 1974). The data reported here, however, have not been corrected for the detector efficiency.

In order to express the electron exposure in terms of current density on the specimen, the electron exposure measurements were made through holes in the specimen support film and were corrected for the final image magnification. A further geometrical correction factor was applied to take into account the slightly higher image magnification in the detector plane. Counting rates were taken at image magnifications which would yield 10^4 counts/sec. Background counts were taken both before and after with the fluorescent screen lowered but all other conditions kept constant. In this experiment, measured background counts were never more than 1% of the total count rate.

The electron diffraction patterns were recorded primarily on Kodak No-Screen X-ray film, but occasionally on Kodak Electron Image plates. The x-ray film was developed according to the procedure of Matricardi et al. (1973) and the lantern slide plates were developed in 1:2 HRP

developer, without antifog, for 5 minutes, a procedure which the manufacturer suggests for maximizing the electron speed.

The radiation damage effect was measured by recording serial electron diffraction patterns of single crystals of catalase. This series of diffraction patterns was spaced over a 20 minute period using current densities ranging from 6×10^{-6} to 2×10^{-5} Amperes/cm^2. Low current densities such as these are not believed to cause substantial specimen heating (Reimer, 1960). This is an important point because a temperature rise of as much as 40°C could cause loss of hydration due to sublimation of the ice (Heide and Grund, 1974), and this would complicate the interpretation of the diffraction results. With current densities such as these and illuminated areas of about 3-4 μ^2, 1-2 minute exposure were necessary for recording usable electron diffraction patterns. Such long exposure times necessarily limit the shortest time interval that can be taken between successive patterns. For this reason, the interval was limited to one minute between the first two patterns and was increased to up to 5 minutes between the last two patterns. The midpoint of the interval during which the diffraction was recorded was used for the purpose of computing the accumulated electron exposure.

The electron diffraction results have been plotted in Fig. 9 to show the resolution remaining in the diffraction pattern as a function of the accumulated electron exposure of the specimen, expressed in Coulombs/cm^2. The results show a decline in the resolution remaining as a function of the logarithm of accumulation exposure. A logarithmic behavior such as this has also been observed in other organic materials

(Salih and Cosslett, 1974).

The scatter in the data points indicates an experimental error of about 30%. It is believed that this error is due primarily to variation in the visibility of the electron diffraction spots. The visibility of a diffraction spot will be reduced if the crystal does not fill the area being illuminated or if the crystal is very thin but not large in extension. For a constant area of illumination, a thick crystal will produce a more visible pattern than a thinner one, up to the point where inelastic scattering and dynamical effects become important. Except for the visibility problem, critical exposure will be independent of the crystal thickness because the stopping power of the 100 keV electrons used remains essentially constant during their passage through the specimen.

Two observations can be made based on the electron diffraction results shown in Fig. 9. First the radiation damage effect in frozen hydrated catalase does not appear to be nearly as great as it is in the hydrated crystals at room temperature. Critical exposure for fading of the electron diffraction pattern to 86 Å resolution at room temperature have been reported to be about 2×10^{-3} Coulombs/cm^2 (Martricardi et al., 1972). This is approximately a factor of 10 less than that reported here for the frozen catalase.

There is some risk in comparing radiation damage data from different laboratories. However, historically the agreement is quite good between the few specimens whose critical exposures have been measured in different laboratories. A factor of two could be considered safe for comparison purposes. Thus differences of greater than a factor of two

Figure 9. Critical exposure for fading of the electron diffraction pattern of frozen, hydrated catalase as a function of the resolution.

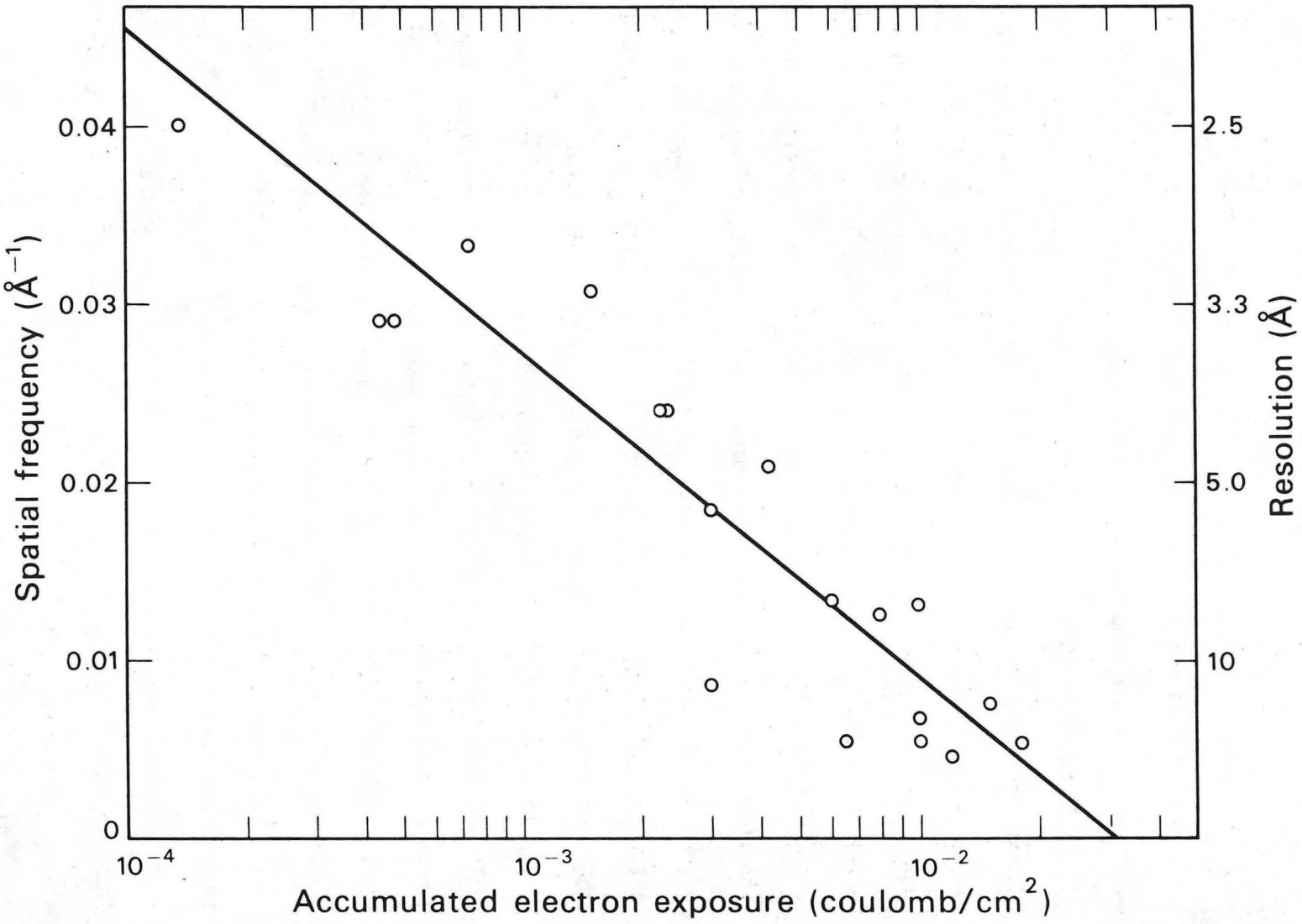

XBL 7412-8174

Fig. 9

can be considered significant. With this in mind, the factor of ten difference reported here between the frozen catalase and the hydrated catalase at room temperature is quite significant.

A possible point for discrepancy between results reported from different laboratories could arise due to difference in detector efficiency. To be strictly correct one should use a primary standard such as a Faraday cage. In the work reported here this was not possible. However, since the data reported here have not been corrected for detector efficiency, this correction if applied, would have the effect of increasing the value for the critical exposure. The critical exposure data reported by Matricardi et al., were taken using the phosphor screen as an electron detector. They report an efficiency of 50% which is quite comparable to that reported in this work for the Li drifted Si detector.

In addition, prior to the installation of our detector system, current densities for diffraction experiments (but not radiation damage experiments) were adjusted using valine as a test specimen (critical exposure = 1.3×10^{-3} Coulomb/cm^2). At current densities where valine faded in 2 min, catalase diffraction was still present after 20 min.

This improvement in critical exposure between the room temperature hydrated catalase and the frozen hydrated catalase may be due in part to a mechanical, supporting action of the ice matrix around the protein. This ice matrix occupies about 50% of the volume of the unit cell in catalase. (Mathews, 1968)

The radiation damage process is believed to occur in two stages (Siegel, 1972). The primary step is bond fracture, which is essentially

temperature independent, and this is followed by molecular rearrangement or diffusion of the fragments that result from the bond fracture process. It is this last step which is believed to be temperature dependent. For a protein molecule in a liquid matrix, molecular rearrangment could occur quite easily. But if the water matrix is solid, then diffusion of molecular fragments could be in effect reduced, and the protein conformation might be maintained up to a higher dose of irradiation.

Previous studies of the effect of low temperature on the critical exposure have given various results. Glaeser et al. (1971) found little improvement in the critical exposure for valine when the temperature was reduced from room temperature to liquid helium temperature. Siegel (1972) in a more extensive study found an improvement in critical exposure in both an aromatic and an aliphatic compound. He also reported a smaller improvement at liquid nitrogen temperature. It can be said, however, that the improvement at liquid helium temperature has never been greater than a factor of 4-5 over room temperature for small organic molecules. The larger effect in the case of hydrated catalase is quite probably a reflection of differences associated with the liquid vs the solid state, which have not been a factor in previous studies.

The second observation that can be made is that the critical exposure for fading of the diffraction pattern to low resolution (15 Å) is only slightly less than that reported for uranyl acetate stained catalase (Glaeser, 1971). The comparison, however ends at that resolution. The reason for this lies in the ability of a negatively stained specimen to reach a final, stable end-point, beyond which no observable changes in

the electron diffraction pattern or image occur (Glaeser, 1971). As can be seen from Fig. 9, this does not occur for the frozen hydrated specimens. No final, stable end point is reached, and indeed, very gross radiation damage effects can occur if the intensity is very high (Taylor and Glaeser, 1973).

C. The Imaging of Hydrated Specimens

The recording of lattice images of unstained, hydrated catalase requires especially delicate techniques because of both the sensitivity of these crystals to electron irradiation and their inherently low contrast. The use of a minimal exposure technique (Williams and Fisher, 1970) is an absolute requirement. A number of techniques for recording lattice images have been tried. The major problems occur in obtaining the correct focus and in locating crystals using low illumination intensities. It has been found to be almost impossible to focus directly on the lattice image itself. To circumvent this difficulty, two techniques were tried: (1) Use of the bright field-dark field image displacement of bend contours resulting from the 3.89 Å Bragg reflection from the surrounding ice, and (2) Focusing on phase contrast granularity of the support film or Fresnel fringes in voids formed in the surrounding ice after some of this ice has been sublimed under the influence of the electron beam.

When an objective aperture is used which stops all the ice diffraction spots except the six hexagonally arranged spots at 3.89 Å spacing, the resulting image of the crystalline ice has both single, dark bend

contours caused by aperturing out all the diffraction spots from spacings smaller than 3.89 Å and pairs of bright field (black) and dark field (white) bend contours ascribable to the 3.89 Å Bragg reflection. The separation between the bright field, dark field pair is given by expression (Budinger,1971)

$$|\vec{\alpha}| = C_s\lambda^3 |\vec{g}|^3 - \Delta f\lambda|\vec{g}| \qquad (1)$$

where $|\vec{a}|$ is the magnitude of the displacement, C_s is the coefficient of spherical aberration, λ is the electron wave length, $\vec{g}$ is the reciprocal spacial frequency, and Δf is the defocus. For a $|\vec{g}|$ of $(3.89\,\text{Å})^{-1}$, the two images will overlap one another at a defocus of 839 Å when $C_s = 1.4$ mm and $\lambda = 0.037$ Å. In principle, having achieved the overlap of the two images, the correct defocus can be selected.

There are several drawbacks to this method of focus assessment. First of all, the precision in obtaining the correct defocus is only about 2000 Å when the focusing is done at a magnification of 5000 x. Secondly, the technique can only be carried out a low magnification because the high current densities necessary to image at high magnification generally cause movement of the bend contours. Last but not least, a bright field-dark field pair is not always present in the region of a catalase crystal.

Although scanning and focusing with this method must be done at low magnification, image recording using x-ray film must be done at magnifications of 30-40,000 x, because of its low emulsion resolution. When the magnification is increased, the focus can be compensated by a previously

determined amount. However, this compensation introduces a further uncertainty in the defocus. With all the problems that this method has, it is remarkable that lattice images can be obtained at all. When this technique was used, lattice images were obtained on the plate 8 out of 10 times.

The second method of focus assessment involved the use of the phase contrast granularity of the surrounding support film or alternatively, Fresnel fringes in voids in the surrounding ice. Voids are formed by focusing the electron beam on the surrounding ice and allowing the ice to partially sublime. When the sublimation is carried to completion, only the support film remains and the phase contrast granularity can then be visualized. It is sometimes necessary to increase the magnification from the value of 30 or 40,000 x , where image recording is done, in order to visualize the granularity. Again, the focus can be adjusted by a known amount when the magnification is reduced for image recording. Precision in obtaining the desired defocus is about 1000 Å by this technique which is acceptable for achieving image resolution down to about 10 Å.

In addition to recording images on Kodak No-Screen X-ray film, Kodak Electron Image Plates (lantern slide) were also used. However to maximize the electron speed of the lantern slide plates, they were developed in 1:2 HRP developer, without anti-fog, for 5 minutes at 20° C. With the x-ray film, useful images can be recorded with specimen exposures of about 2×10^{-3} Coulombs/cm^2 at a magnification of 40,000 x. The image resolution of this emulsion for recording a periodic object with high contrast has been measured to be 30 μ (Kuo, 1975). This number is obtained

by recording images of negatively stained catalase at various magnifications and determining the highest resolution recorded on the plate taken at successively lower magnifications. The resolution on the plate times the image magnification is the emulsion resolution, also called the grating resolution. With conventional electron image plates, the grating resolution is about 10 μ but the specimen exposures necessary to record an image are about ten times greater than are necessary with x-ray film.

In Fig. 10 is shown an image, recorded on a conventional lantern slide plate, of an unstained, unfixed catalase crystal embedded in ice. In the low magnification image shown in Fig. 10a, bend contours can be seen in the surrounding ice which extend partially across the crystal. The fact that they do not extend entirely across the crystal is implicit proof that the support films are in contact with the surface of the crystal, thus minimizing the thickness of the ice above the specimen. Figure 10b is an optical diffraction pattern taken from this area. The single weak spot in the second order of the 68 Å repeat indicates that a lattice resolution of 34 Å is present in the image.

In Fig. 11, an image of a catalase crystal recorded on x-ray film is shown. The optical diffraction pattern of this image, shown in the insert, has a single weak spot in the third order of the 68 Å repeat at a resolution of about 22 Å.

It was interesting to attempt to measure the radiation damage effect in frozen, hydrated catalase using images rather than diffraction patterns. The reason for this was to see if there was any change in the critical exposure under imaging conditions. Images are recorded under

Figure 10. Electron micrograph of a catalase crystal embedded in ice. (a) A relatively low magnification image showing bend contours in the surrounding ice and the complete absence of frost particles on the specimen. (b) An enlargement showing the lattice of the protein crystal. An optical diffraction pattern from this area is shown in the inset.

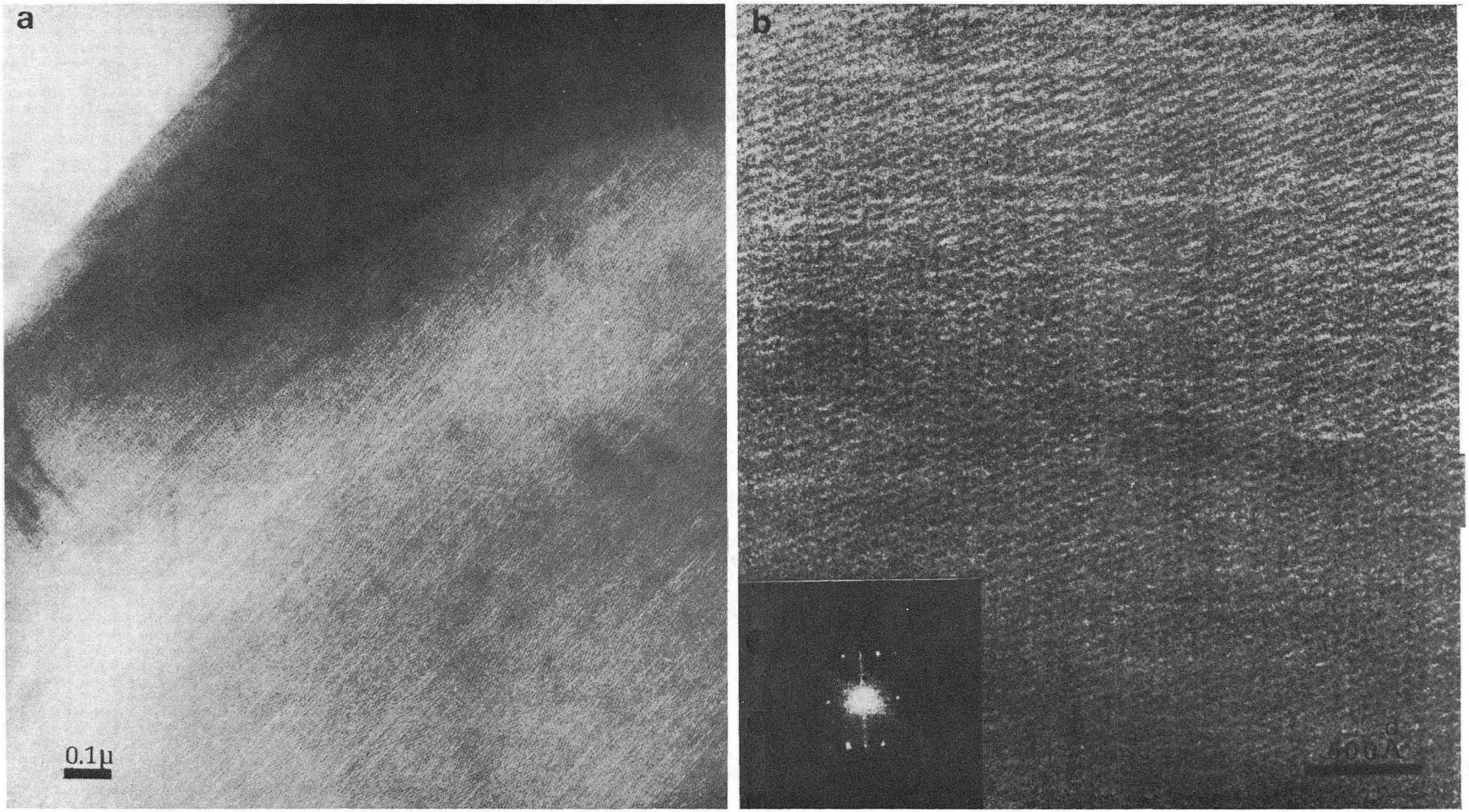

XBB 751-843

Fig. 10

Figure 11. Lattice image of a frozen, unstained, unfixed catalase crystal recorded on No-Screen X-ray film using minimal exposure. One weak spot in the third order of the 68 Å repeat is present in the optical diffraction pattern (inset) indicates a resolution of 21 Å is present in the image.

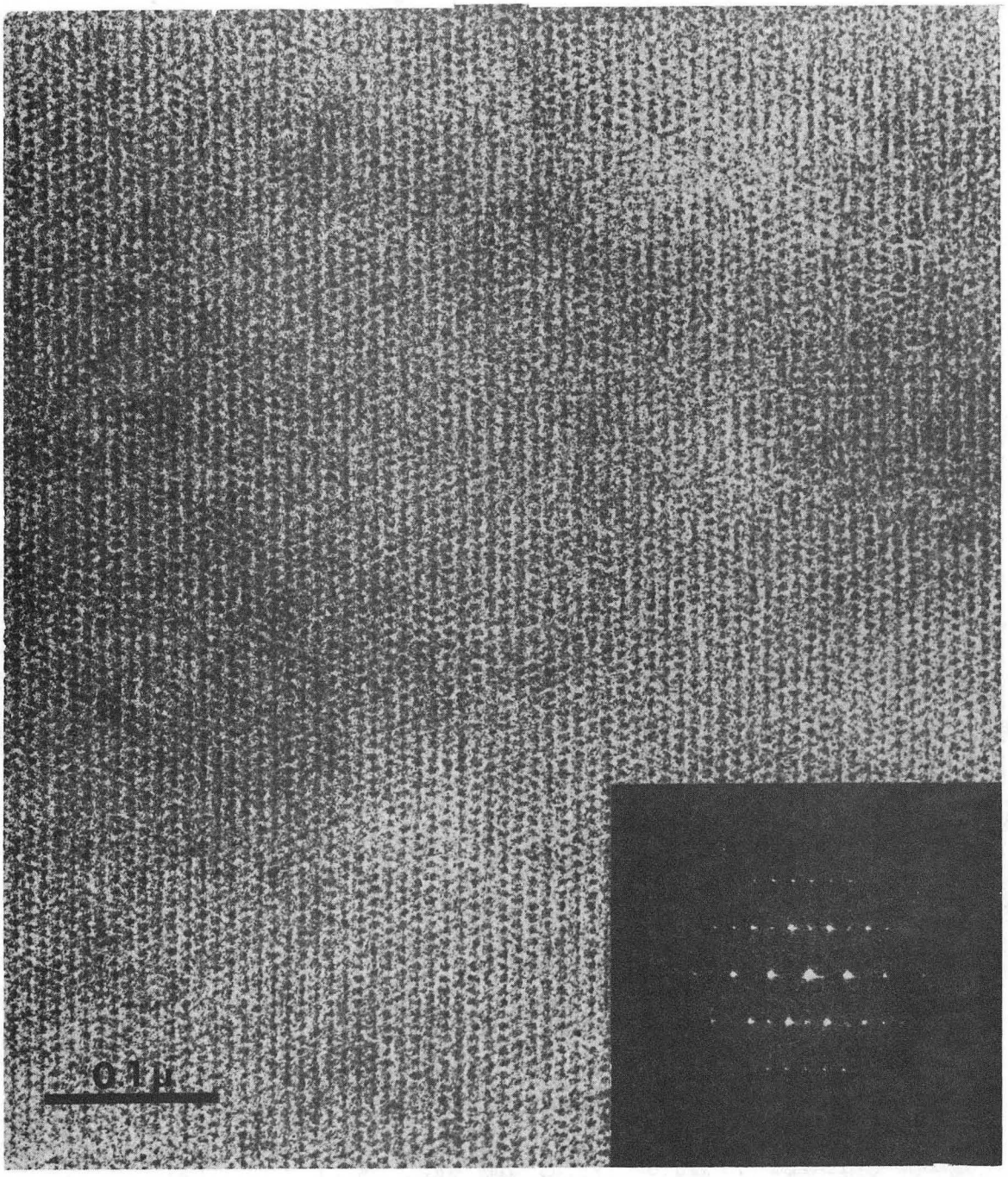

XBB 751-850

Fig.11

somewhat different conditions than those used for diffraction experiments. First of all, the beam area is much larger and secondly, the current densities are about 20 times greater. There are some drawbacks to this approach because it is generally easier to record a high resolution diffraction pattern than a high resolution image. The results have a more "local" character because the optical diffraction patterns which are used to determine image resolution are taken from areas which are about ten times smaller than those used for obtaining electron diffraction patterns. Thus changes occurring in small areas of the specimen, which would be averaged out in a diffraction pattern, are more easily discovered.

The experimental technique in the imaging experiment is quite analogous to that used in the electron diffraction experiment. A series of three images are recorded of each crystal, using 10 second exposures with a 15 second period taken between successive images. Again, the midpoint of the recording interval was used to compute the accumulated exposure. Of course the first image was obtained using the minimal exposure technique. Current density at the specimen in this case was 6×10^{-4} Amperes/cm^2.

Optical diffraction patterns obtained from a series of images of one hydrated catalase crystal are shown in Fig. 12. Pairs of optical diffraction patterns are shown, from opposite ends of the same crystal but from the same plate. The lack of circular symmetry in the optical diffraction patterns has been a frequent, though unexpected effect. It seems certain in this instance, that the asymmetry is not due to specimen

drift or to astigmatism. Specimen drift undoubtedly occurs in some images when the specimen holder is not in thermal equilibrum with the cold stage. However, specimen drift or astigmatism must cause a pair of optical diffraction patterns obtained from different parts of the same plate to be asymmetric in the same manner. The optical diffraction pattern on the left side of Fig. 12a shows the second order of the 68 Å repeat (i.e. 34 Å) but only the second order of the 172 Å repeat (i.e. ~86 Å). Because of the crystal symmetry, only even reflections are allowed along this zone axis. The diffraction pattern on the right has only the first order of the 68 Å repeat but the sixth order of the 172 Å (i.e. ~29 Å). Since these reciprocal lattice axis are perpendicular it can be concluded that neither drift nor astigmatism are limiting the resolution and causing the observed asymmetry.

The observed asymmetry could also be caused by a tilting of catalase crystal so that its face is no longer perpendicular to the electron beam. Such a tilt would give rise to an electron diffraction pattern, which of course gives rise to the final image, that no longer has circular symmetry. We have not observed tilting effects such as these in electron diffraction patterns of catalase, possibly due to the fact that electron diffraction data are taken from areas which are much larger than areas used in the optical diffraction data of Fig. 12. Electron diffraction data reported here were taken from areas of about $3\,\mu^2$ while the optical diffraction patterns came from areas of about $0.3\,\mu^2$ (referred to the object). Thus an averaging effect over several slightly different orientations may be occurring in the electron diffraction experiments.

Figure 12. Critical exposure for frozen hydrated catalase measured by deterioration of the image resolution. (a) A pair of optical diffraction patterns from an image of a catalase crystal after 2.8×10^{-3} Coulomb/cm^2 accumulated exposure. (b) Optical diffraction patterns from the second image of the same crystal after 1.6×10^{-2} Coulomb/cm^2 accumulated exposure. (c) Optical diffraction patterns from the third image of the same crystal after 3.0×10^{-2} Coulomb/cm^2 accumulated exposure. The lack of circular symmetry in the optical diffraction patterns is believed to be due to local tilting (warping) of the crystal.

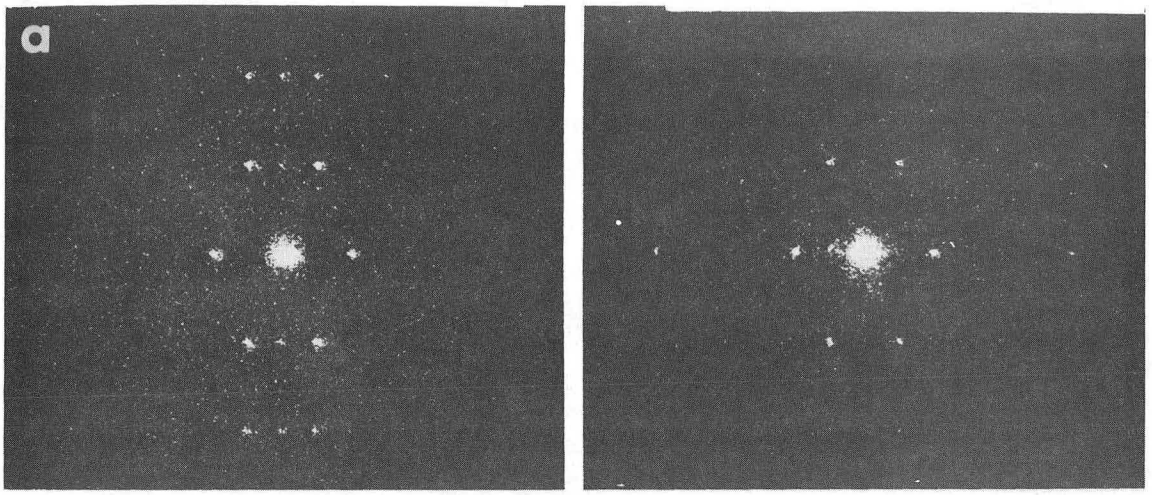

Accumulated exposure = 2.8×10^{-3} C/cm^2

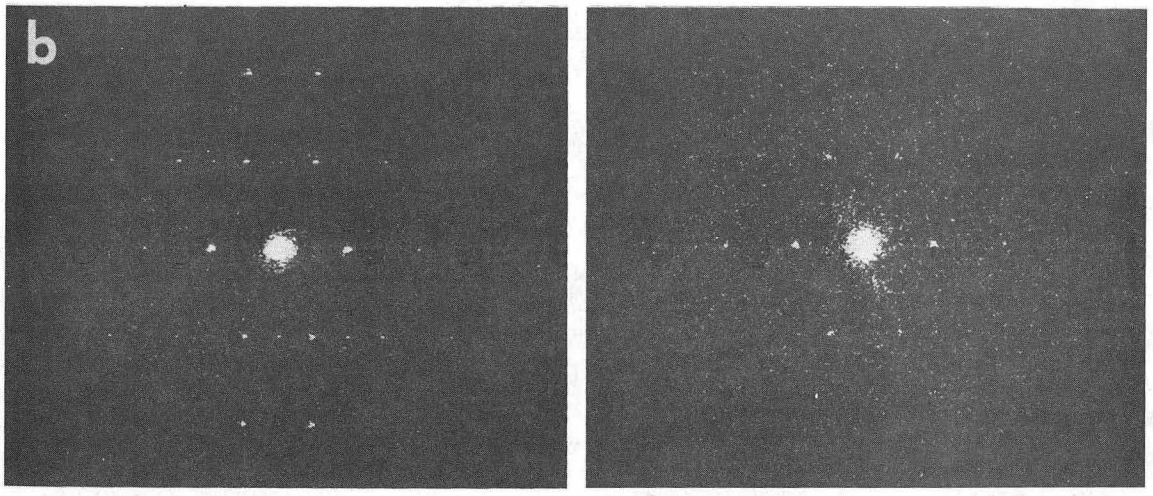

Accumulated exposure = 1.6×10^{-2} C/cm^2

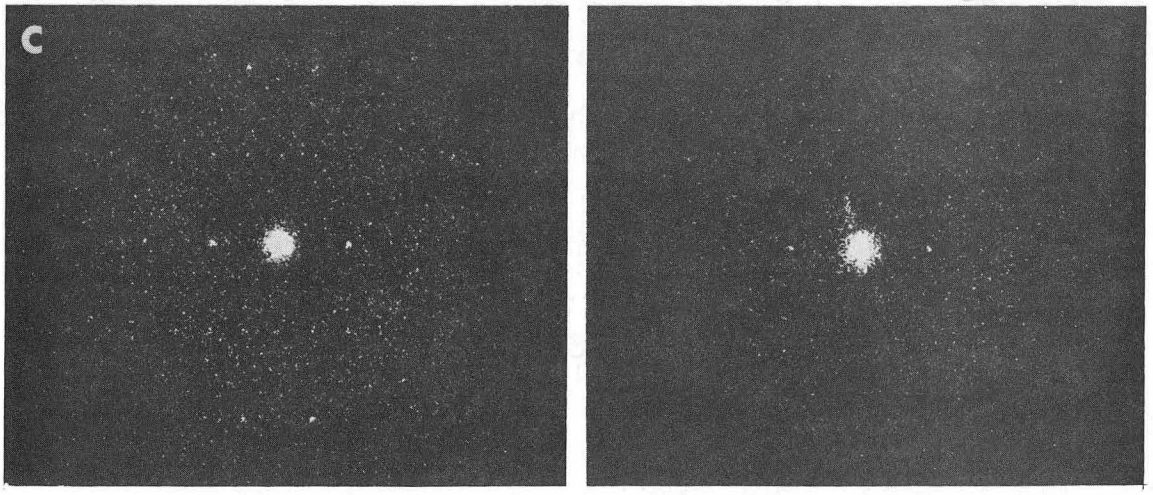

Accumulated exposure = 3.0×10^{-2} C/cm^2

Fig. 12

XBB 751-844

Also it may be possible that a small amount of specimen heating due to the higher current densities used in imaging is causing this effect. Even when the specimen is scanned at low magnification using low beam intensity, bend contours in the surrounding ice can be seen to vary with time. This effect is known to be caused by changes in the orientation of the ice.

Some local specimen tilt could also be introduced within the catalase crystals if the bulk ice surrounding them underwent a phase change from the vitreous to the crystalline state while the temperature of the specimen holder was increased to that of the cold stage. This tilt would arise from the different densities between the two ice phases. Because of the constraints in the plane of the specimen, this expansion between the glassy and crystalline ice would likely cause some buckling of the specimen.

The optical diffraction patterns shown in Fig. 12 are in agreement with the electron diffraction results of Fig. 9 at low resolution. It is interesting to point out the increase in the number of diffraction spots in Fig. 12b over Fig. 12a. This is further evidence of a change in specimen orientation occurring between exposures. There is a reduction in diffraction intensity in Fig. 12b relative to 12a which is evidence of crystal disordering. From Fig. 9, by extrapolating the data, the critical exposure for complete fading of the electron diffraction pattern is 3×10^{-2} Coulombs/cm^2. In Fig. 12c, even after a specimen exposure of 3×10^{-2} Coulombs/cm^2, the 34 Å diffraction spots are still present, although greatly reduced in intensity.

D. Contrast in Unstained, Hydrated Specimens

Contrast in images of biological specimens is important from the standpoint of radiation damage. This functional dependence of radiation damage on contrast can be derived from the equation (Rose, 1948)

$$N(d) \geq (5)^2/f\, d^2\, C(d)^2 \qquad (2)$$

where C(d) is the image contrast, which may depend on the resolution, d is the resolution, f is an efficiency factor for electron detection and electron optical utilization, N(d) is the specimen exposure, expressed in $e^-/Å^2$, required to resolve image detail at resolution d, and 5 is an emperical factor expressing the signal to noise ratio necessary for visual detection. A reduction in contrast increases quadratically the number of electrons required to statistically define image detail at a given resolution. However, radiation damage places an additional restraint on N(d) such that it must also be less than the critical exposure for that resolution.

The contrast in lattice images of unstained, unfixed, hydrated catalase has been measured by taking a one dimensional densitometer scan of the image. This was done using the Joyce-Loebl Double Beam Recording Microdensitometer. Using this method, the contrast can then be calculated from the expression

$$\text{contrast} = \Delta C/\langle C \rangle \qquad (3)$$

where ΔC is the periodic fluctuation in the optical density and $\langle C \rangle$ is the average optical density.

In Fig. 13a is a lattice image of a catalase crystal, whose optical diffraction pattern is shown in the inset. The resolution in this image is 21.5 Å as is demonstrated by the presence of the eighth order of the 172 Å repeat. In Fig. 13b is shown the one dimensional densitometer line scan of this image, scanned parallel to the 172 Å repeat. The average optical density of the plate (minus the optical density of the film itself) is 2.0 and the change in optical density due to the lattice image is 0.24 which results in an image contrast of 11%.

The constraints on obtaining the necessary image statistics given by Eq. 2 are severe especially when it is necessary to obtain a statistically defined image of each point in the specimen. For instance, if values of the contrast as determined here for catalase crystals are taken (10%) and a reasonable value is assumed for the electron utilization factor (25%), then from Eq. 2, for a image resolution of 10 Å, an exposure of 100 $e^-/Å^2$ is necessary to obtain a statistically defined image. If the critical exposure measurements for catalase can be used as an example, structure at 10 Å will no longer be present when the specimen exposure exceeds 5 $e^-/Å^2$ (8×10^{-3} Coulomb/cm^2). Thus, it seems unlikely that high resolution microscopy will be possible on small, free standing particles such as single enzymes. The imaging of such specimens appears even more impossible if one realizes that contrast in free standing particles will be less than in the crystalline specimens used in this study.

However, for a periodic object it is only necessary that the image statistics summed over the entire crystal satisfy Eq. 2. For the example given above, the required image statistics might be obtained by spatial

averaging over a mere 20 unit cells. Such a method is known as the Statistically Noisy, Averaged Picture (SNAP-shot) technique (Glaeser et al., 1971).

Figure 13. (a) An image of an unstained hydrated catalase crystal of unknown thickness recorded on No Screen X-ray film. The optical diffraction pattern shown in the insert contains the 8th order of the 172 Å repeat for an image resolution of 21.5 Å. (b) A densitometer trace taken in a direction parallel to the 172 Å repeat. From this densitometer trace an image contrast of 11% can be calculated.

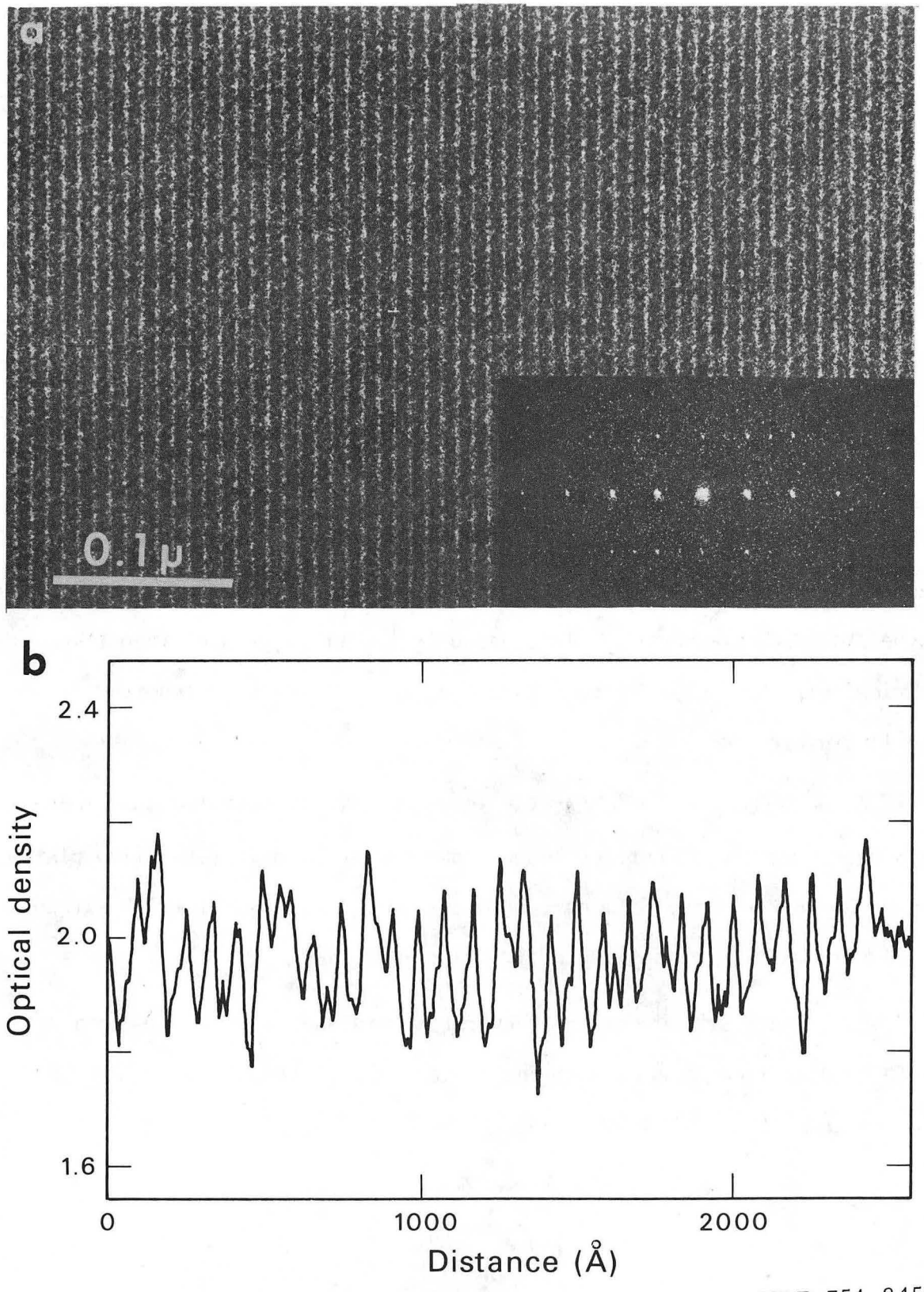
a
0.1μ
b
2.4
2.0
1.6
Optical density
0
1000
2000
Distance (Å)
XBB 751-845

Fig. 13

IV. SUMMARY

1. Techniques for preparing frozen, thin, sandwiched specimens for electron microscopy have been described. In addition techniques have been described for introducing a frozen specimen into the electron microscope which prevent frost formation and specimen warning.

2. Electron diffraction has been used to show that preservation of crystalline structure in the frozen state is excellent.

3. The radiation damage effect has been measured in frozen, hydrated catalase crystals using electron diffraction. The critical exposure for complete fading of the electron diffraction pattern was found to be 3×10^{-2} Coulombs/cm^2. This value is ten times greater than the critical exposure of hydrated catalase at room temperature reported in the literature.

4. Techniques for obtaining images of frozen hydrated specimens have been described. Lattice images recorded on both lantern slide plates and on No-Screen X-ray film have been obtained, the best of which extend to 21 Å resolution by optical diffraction tests.

5. Contrast in unstained, hydrated catalase crystals has been determined by direct densitometry of the image. The contrast was found to be greater than 10%.

V. CONCLUSIONS

The work of this thesis has been that of describing the development of a frozen specimen technique that will ultimately lead to the study of unstained, hydrated biological structure in the electron microscope. The advantage that the frozen specimen technique has over the room temperature hydration methods are that (a) Brownian motion is completely eliminated with frozen specimens but could be a problem with liquid hydration techniques. (b) Frozen specimens are ten times more resistent to radiation damage than are hydrated specimens at room temperature. (c) The frozen specimen technique is as easy to use as is the negative staining technique. (d) The specimen thickness does not change due to evaporation or condensation of water vapor. (e) The technique requires negligible instrument modification (a cold stage and methodology for introducing a frozen specimen to prevent frost formation). (f) In closed chamber, thin window hydration stages, rupturing of the windows can occur. (Inorder to reduce the chances of window rupture, the windows can be made thicker but this contributes to a loss in image contrast and resolution). With frozen specimens, the sandwiching windows can be as thin as 20 Å each without rupturing, if a secondary reticulate support film is used. (g) There are negligible problems of stage regulation involved when using frozen specimens as compared with the delicate regulation of water vapor pressure and stage temperature that is involved in the operation of the differentially pumped hydration stage.

In addition to being suitable for electron diffraction work it has been shown here that the imaging of unstained hydrated protein crystals is also possible. With such specimens the contrast is relatively good and the large number of repeats makes it possible to average the data to obtain images that are statistically well determined for each resolution. In addition there is no reason why the techniques could not be applied to periodic membranes such as gap junctions. In this case however, the contrast is likely to be much as less because these specimens are much the thinner.

A more intriging problem is the possibility of studying at high resolution specimens which can be categorized as free standing particles. These include single virus particles and even enzyme complexes. In these instances, the radiation damage is a much more severe limitation to high resolution studies. With free standing particles the problem is one of averaging inorder to build up the statistics necessary to define image detail at a given resolution. With some viruses such as TMV there are reasonable number of repeats available for averaging but for other particles there may only be one repeat. Some hope may exist for this area through the use of cross correlation functions as has been suggested by Frank (1974). With this method one could average over particles which were incoherently oriented rather than summing over unit cells in a coherent crystal. Even with this technique assuming it is practical, one would likely need some symmetry in the specimen in order to define orientation.

In the near future it would appear that the best results will be obtained with specimens whose structure is composed of a periodic repetition of a basic unit. In addition to the numerous enzyme that can be crystallized in a form suitable for electron microscopy, some biological membranes and many viruses are periodic. Moreover, there are some interesting specimens which cannot be crystallized in vitro but can crystallize within the cell. These include ribosome crystals which are found in chick embryo cells (Byers, 1967) and in Entamoeba invadiens (Barker and Deutsch, 1958) and Tobacco Mosaic Virus crystals (Wilkens et al., 1950). It may be possible to obtain frozen thin sections of these specimens and observe them in the hydrated state, thus avoiding the problem of specimen isolation.

ACKNOWLEDGMENTS

I would like to express my appreciation to Professor Robert M. Glaeser for suggesting this project and for providing ideas throughout its development. In addition I would like to thank the various members of our research group for many helpful discussions throughout this project. These include Ivy Kuo, David Grano, Bing K. Jap, and Wah Chiu. The able work of Robert Nordhausen in keeping our microscope in excellent condition is acknowledged. In addition I would like to thank E. F. Dowling who assisted in the construction of the apparatus used in addition to instructing myself on how to use the machine shop. The drawings by John Flambard are greatly appreciated.

Finally, and above all I would like to acknowledge the support of my wife Dianne who has sacrificed much in the last few years to bring this about.

This investigation was supported by USPHS Training Grant No. 5 T01 GM 00829 from the National Institute of General Medical Sciences, and in part by the U. S. Energy Research and Development Administration.

APPENDIX I

In this Appendix are shown the images from which the optical diffraction patterns in Fig. 12 were taken. The images are oriented so that the left side of the image corresponds to the optical diffraction patterns on the left in Fig. 12.

Figure 14. A series of images of an unstained, hydrated catalase crystal after various electron exposures. (a) Image of the crystal after 2.8×10^{-3} Coulomb.cm^2 accumulated exposure. (b) Image of the crystal after 1.6×10^{-2} Coulomb/cm^2 accumulated exposure. (c) Image after 3.0×10^{-2} Coulomb/cm^2 accumulated exposure. The patchy spots on the images are believed to be due to frost contamination forming on the specimen inside of the column of the microscope. Optical diffraction patterns from these images are shown in Fig. 12.

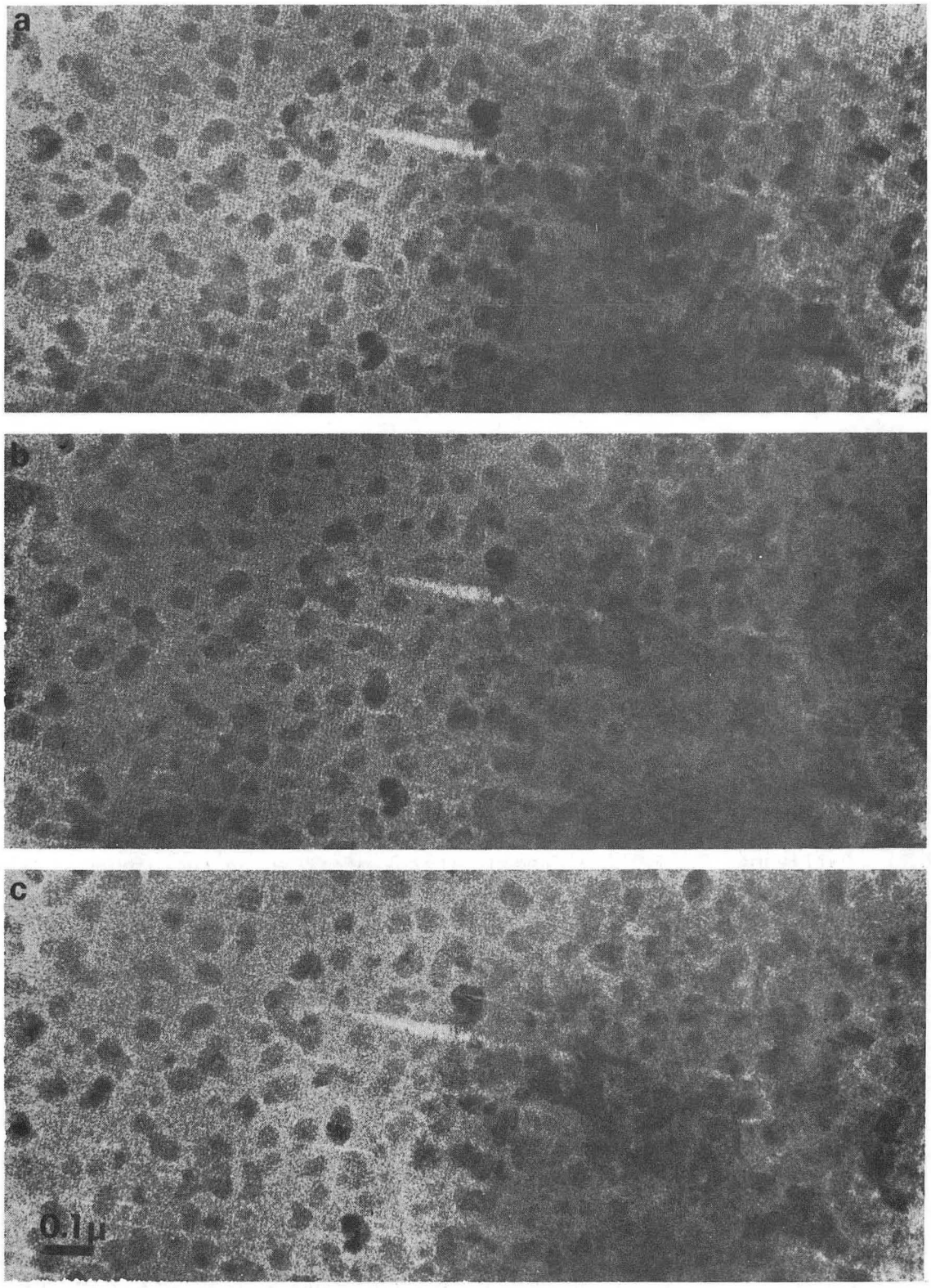

XBB 754-2830

Fig. 14

REFERENCES

1. Abrams, I. M. and J. W. McBain. 1944. A closed cell for electron microscopy. J. Appl. Phys. 15, 607.

2. Barker, D. C. and K. Deutsch. 1958. The chromatoid body of Entamoeba invadiens. Exp. Cell Res. 15, 604.

3. Blackman, M. and N. D. Lisgarten. 1959. Electron diffraction investigations into the cubic and other structural forms of ice. Adv. Phys. 7, 189.

4. Bradley, D. E. 1965. The preparation of specimen support films. In Techniques for Electron Microscopy. D.H. Kay ed. F. A. Davis Co., Philadelphia, p58.

5. Budinger, T. F. 1971. Transfer function theory and image evaluation in biology: Applications in electron microscopy and nuclear medicine. Ph.D. Thesis. University of California, Berkeley.

6. Bullivant, S. 1970. Present status of freezing techniques. In Some Biological Techniques in Electron Microscopy. D. F. Parsons ed. Academic Press, New York. p101.

7. Byers, B. 1967. Structure and formation of ribosome crystals in hypothermic chick embryo cells. J. Mol. Biol. 26, 155.

8. Dowell, L. G., S. W. Moline, and A. P. Rinfret. 1962. A low temperature x-ray diffraction study of ice structures formed in aqueous gelatin gels. Biochim. Biophys. Acta 59, 158.

9. Frank, J. 1974. Digital correlation methods in electron microscopy. Unpublished.

10. Fraser, R. D. B. and T. P. MacRae. 1973. Conformation in Fibrous Proteins and Related Synthetic Polypeptides. Academic Press, New York.

11. Glaeser, R. M. 1971. Limitations to significant information in biological electron microscopy as a result of radiation damage. J. Ultrastruct. Res. 36, 466.

12. Glaeser, R. M., I. Kuo, and T. F. Budinger. 1971. Method for processing of periodic images at reduced levels of electron irradiation. Proc. 29th Meeting Electron Microscopy Soc. Am. p466.

13. Glaeser, R. M., V. E. Cosslett, and U. Valdre. 1971. Low temperature electron microscopy: radiation damage in crystalline biological materials. J. Microscopie 12, 133.

14. Harris, R. J. C. 1964. Biological Applications of Freezing and Drying. Academic Press, New York.

15. Hass, G. 1950. Preparation, structure, and applications of thin films of silicon monoxide and titanium dioxide. J. Am. Ceram. Soc. 33, 353.

16. Heide, H. G. and S. Grund. 1974. Eine Tiefkuhlkette zum uberfuhren von wasserhaltigen biologischen Objekten ins Electronenmikroskop. J. Ultrastruct. Res. 48, 259.

17. Hoppe, W., R. Langer, G. Knesch, and Ch. Poppe. 1968. Protein-Kristallstrukturanalyse mit Elektronenstrahlen. Naturwiss. 55, 333.

18. Howitt, D. G. (Materials Science Dept., University of California, Berkeley, CA 94720) Private communication, 1974.

19. Hui, S. W. and D. F. Parsons. 1974. Electron diffraction of wet biological membranes. Science 184, 77.

20. Jap, B. K. 1975. Dynamical electron scattering approximation and their validity domains in electron microscopy. Thesis. University of California, Berkeley.

21. Joy, R. T. 1973. The electron microscopical observation of aqueous biological specimens. Adv. Opt. Elect. Microsc. 5, 297.

22. Kuo, I. 1975. Electron microscopy at reduced levels of irradiation. Thesis, University of California, Berkeley.

23. Langer, R., Ch. Poppe, H. J. Schramm, and W. Hoppe. 1974. Embedding and thin sectioning of x-ray aligned protein crystals. Proc. 8th Int. Congress of Electron Microscopy, Canberra. 2, 172.

24. Longley, W. 1967. The crystal structure of bovine liver catalase: a combined study by x-ray diffraction and electron microscopy. J. Mol. Biol. 30, 323.

25. Mathews, B. W. 1968. Solvent content of protein crystals. J. Mol. Biol. 33, 491.

26. Matricardi, V. R., G. Wray, and D. F. Parsons. 1972. Evaluation of emulsions and other recording media for 100 and 1000 keV electron microscopes. Micron 3, 526.

27. Matricardi, V. R., R. C. Moretz, and D. F. Parsons. 1972. Electron diffraction of wet proteins: catalase. Science 177, 268.

28. Meryman, H. T. ed. 1966. Cryobiology. Academic Press, New York.

29. Moretz, R. C., C. K. Akers, and D. F. Parsons. 1969a. Use of Small angle x-ray diffraction to investigate disordering of

membranes during preparation for electron microscopy, I. Osmium tetroxide and potassium permanganate. Biochim. Biophys. Acta 193, 1.

30. Moretz, R.C., C. K. Akers, and D. F. Parsons. 1969b. Use of small angle x-ray diffraction to investigate disordering of membranes during preparation for electron microscopy. Biochim. Biophys. Acta 193, 12.

31. Parsons, D. F. 1966. Electron diffraction of helical forms of polyribonucleotides and polyamino acids. Proc. 6th Int. Cong. Electron Microscopy, Kyoto 1, 212.

32. Parsons, D. F. 1974. Structure of wet specimens in electron microscopy. Science 186, 407.

33. Parsons, D. F. and U. Martius. 1964. Determination of the alpha helix configuration of poly-γ-benzyl-L-glutamate by electron diffraction. J. Mol. Biol. 10, 530.

34. Parsons, D. F., V. R. Matricardi, R. C. Moretz, and J. N. Turner. 1974. Electron microscopy and diffraction of wet unstained and unfixed biological objects. Adv. Biol. Med. Phys. 15, 162.

35. Reimer, L. 1965. Irradiation changes in organic and inorganic objects. Lab. Invest. 14, 1082.

36. Rose, A. 1948. Television pickup tubes and the problems of vision. Adv. Electronics 1, 131.

37. Salih, S. M. and V. E. Cosslett. 1974. Some factors influencing radiation damage in organic substances. Proc. 8th Int. Congr. Electron Microscopy, Canberra 2, 670.

38. Siddal, G. 1960. Vacuum deposition of dielectric films for capacitors. Vacuum 1, 274.

39. Siegel, G. 1972. Der Finfluss tiefer Temperaturen auf die Strahlenschadigung von organischen Kristallen durch 100 keV Electronen. Z. Naturforsch. 27a, 325.

40. Smith, A. U. 1961. Biological Effects of Freezing and Supercooling. (Monograph No. 9 of the Physiological Soc.). Edward Arnold, London.

41. Taylor, K. A. and R. M. Glaeser. 1973. Hydrophilic support films of controlled thickness and composition. Rev. Sci. Instrum. 44, 1546.

42. Unwin, P. N. T. and R. Henderson. 1975. Molecular structure determined by "non-destructive" electron microscopy of unstained specimens. In press.

43. Wilkins, M. H. F., A. R. Stokes, W. E. Seeds, and G. Oster. 1950. Tobacco Mosaic Virus crystals and three dimensional microscopic vision. Nature 166, 127.

44. Williams, R. C. (Molecular Biology and Virus Laboratory, University of California, Berkeley, CA 94720) private communication, 1973.

45. Williams, R. C. and H. W. Fisher. 1970. Electron microscopy of Tobacco Mosaic Virus under conditions of minimal beam exposure. J. Mol. Biol. 52, 121.

45. Williams, R. C. and R. M. Glaeser. 1972. Ultrathin carbon support films for electron microscopy. Science 175, 1000.

TECHNICAL INFORMATION DIVISION
LAWRENCE BERKELEY LABORATORY
UNIVERSITY OF CALIFORNIA
BERKELEY, CALIFORNIA 94720